DOI: 10.1111/tmi.14105

RESEARCH ARTICLE

Improved genetic screening with zygosity detection through multiplex high-resolution melting curve analysis and biochemical characterisation for G6PD deficiency

Usa Boonyuen[1] | Beatriz Aira C. Jacob[1] | Kamonwan Chamchoy[2] | Natnicha Pengsuk[1] | Sirinyatorn Talukam[1] | Chanya Petcharat[1] | Emily R. Adams[3] | Thomas Edwards[3] | Kobporn Boonnak[4] | Syazwani Itri Amran[5] | Nurriza Ab Latif[5] | Naveen Eugene Louis[5]

[1]Department of Molecular Tropical Medicine and Genetics, Faculty of Tropical Medicine, Mahidol University, Bangkok, Thailand

[2]Princess Srisavangavadhana Faculty of Medicine, Chulabhorn Royal Academy, Bangkok, Thailand

[3]Centre for Drugs and Diagnostics Research, Liverpool School of Tropical Medicine, Liverpool, UK

[4]Department of Immunology, Faculty of Medicine Siriraj Hospital, Mahidol University, Bangkok, Thailand

[5]Department of Biosciences, Faculty of Science, Universiti Teknologi Malaysia (UTM), Johor Bahru, Malaysia

Correspondence
Usa Boonyuen, Department of Molecular Tropical Medicine and Genetics, Faculty of Tropical Medicine, Mahidol University, Bangkok, Thailand.
Email: usa.boo@mahidol.ac.th; usa.boo@mahidol.edu

Abstract

Accurate diagnosis of glucose-6-phosphate dehydrogenase (G6PD) deficiency is crucial for relapse malaria treatment using 8-aminoquinolines (primaquine and tafenoquine), which can trigger haemolytic anaemia in G6PD-deficient individuals. This is particularly important in regions where the prevalence of G6PD deficiency exceeds 3%–5%, including Southeast Asia and Thailand. While quantitative phenotypic tests can identify women with intermediate activity who may be at risk, they cannot unambiguously identify heterozygous females who require appropriate counselling. This study aimed to develop a genetic test for G6PD deficiency using high-resolution melting curve analysis, which enables zygosity identification of 15 *G6PD* alleles. In 557 samples collected from four locations in Thailand, the prevalence of G6PD deficiency based on indirect enzyme assay was 6.10%, with 8.08% exhibiting intermediate deficiency. The developed high-resolution melting assays demonstrated excellent performance, achieving 100% sensitivity and specificity in detecting *G6PD* alleles compared with Sanger sequencing. Genotypic variations were observed across four geographic locations, with the combination of c.1311C>T and c.1365-13T>C being the most common genotype. Compound mutations, notably *G6PD* Viangchan (c.871G>A, c.1311C>T and c.1365-13T>C), accounted for 15.26% of detected mutations. The high-resolution melting assays also identified the double mutation *G6PD* Chinese-4 + Canton and *G6PD* Radlowo, a variant found for the first time in Thailand. Biochemical and structural characterisation revealed that these variants significantly reduced catalytic activity by destabilising protein structure, particularly in the case of the Radlowo mutation. The refinement of these high-resolution melting assays presents a highly accurate and high-throughput platform that can improve patient care by enabling precise diagnosis, supporting genetic counselling and guiding public health efforts to manage G6PD deficiency—especially crucial in malaria-endemic regions where 8-aminoquinoline therapies pose a risk to deficient individuals.

KEYWORDS
G6PD deficiency, genotype, high-resolution melting, mutations, structural stability

Sustainable Development Goal: Good Health and Wellbeing

INTRODUCTION

Glucose-6-phosphate dehydrogenase (G6PD) deficiency is an erythro-enzymopathy present in approximately 500 million people worldwide, caused by mutations in the *G6PD* gene that alter catalytic activity or structural stability of the enzyme [1–3]. The reaction catalysed by G6PD is coupled with the formation of reduced nicotinamide adenine dinucleotide phosphate (NADPH), a crucial reducing power in cellular oxidative defence mechanisms [4]. Since mature erythrocytes do not contain mitochondria, G6PD-deficient red blood cells are limited in their ability to generate NADPH at a normal rate, leading to increased vulnerability to haemolysis [5]. This may clinically present as chronic non-spherocytic haemolytic anaemia in severe deficiency, but the more common symptom, acute haemolytic anaemia, could be triggered by infections or exposure to certain food and drugs. Strong regulatory warnings against medications with high oxidative potential such as rasburicase, dapsone, primaquine and tafenoquine have been issued in G6PD-deficient patients since these may cause potentially fatal haemolysis [6]. In particular, treatment of malaria using primaquine and tafenoquine becomes challenging as it has to balance the need to treat the malaria infection effectively while avoiding the risk of severe haemolysis in individuals with G6PD deficiency. This often requires careful monitoring, adjusting drug dosages, or sometimes avoiding medications in favour of alternative treatments. G6PD deficiency also subjects newborns to an increased susceptibility to hyperbilirubinemia which may rapidly progress to kernicterus, a life-threatening neurological dysfunction [7]. Diagnosis of G6PD deficiency is therefore recommended to guide drug administration and early intervention for infants at risk of severe jaundice [6, 8]. Measurement of NADPH formation by ultraviolet–visible spectrophotometry at 340 nm is considered the reference diagnostic standard to determine G6PD activity [9]. Phenotypic assays such as the quantitative CareStart™ G6PD Biosensor and the qualitative fluorescent spot test (FST) are commonly used for point-of-care needs [10].

The *G6PD* gene is located on the X chromosome; therefore, males can be either hemizygous G6PD normal or G6PD-deficient, and females can be homozygous G6PD normal, homozygous G6PD-deficient, or heterozygous G6PD-deficient. Females are subjected to X-chromosome inactivation or lyonization, resulting in varying proportions of G6PD normal and G6PD-deficient red blood cells in heterozygotes [11–13]. This implies a G6PD activity spanning from normal to deficient, which poorly correlates with haemolytic toxicity in heterozygous females, rendering them highly susceptible to drug-induced haemolysis. In addition, haematological factors such as platelet count, leukocyte count and recent haemolysis or blood transfusion affect enzyme activity [6]. Thus, assessment of G6PD deficiency status based on phenotypic tests alone might be particularly unreliable in patients and neonates for whom accurate G6PD deficiency status is crucial.

To avoid adverse reactions, genetic tests are being developed to complement phenotypic results and support accurate diagnosis [6, 14, 15]. Genotypic assays for *G6PD* allele detection include restriction fragment length polymorphism [16], amplification refractory mutation system [17], high-resolution melting (HRM) curve analysis [18], the commercially available DiaPlexC™ G6PD Genotyping Kit, and DNA sequencing as the gold standard. However, these methods are not appropriate for large-population screening due to their time-consuming, low throughput, costly and tedious nature [19–21]. Previous HRM assays were able to determine the zygosity of *G6PD* variants; however, these methods can only detect one to two mutations in one reaction [18, 22]. Fan et al. (2018) devised an HRM assay to detect six variants in four reactions, but the results were complicated to analyse [21]. The HRM method has been developed for straightforward data interpretation to detect 15 common *G6PD* variants found in Asian populations through generating PCR amplicons of distinct melting temperatures in four reactions. This multiplexed method has remarkable sensitivity and specificity, making it suitable for population surveillance [23, 24].

In Thailand, more than 20 *G6PD* genotypes comprising single and double missense, synonymous and intronic mutations, as well as small in-frame deletions have already been identified in the country [25–30]. The predominance of heterozygous G6PD-deficient females among the Thai population stresses the importance of integrating both phenotypic and genotypic tests for much more informed clinical decisions [31–36]. This also facilitates the establishment of genotype–phenotype correlations in order to provide dependable enzyme activity values associated with the prevalent *G6PD* variants in the population [37]. Biochemical analysis of such variants provides further information regarding the molecular mechanisms of G6PD deficiency linked with severe clinical presentations and addresses the proportion of variants with unknown or uncertain function [38–40].

This study was conducted to determine the prevalence of G6PD deficiency, as well as the frequencies of *G6PD* mutations in four different locations in Thailand. G6PD phenotyping was performed using an indirect enzyme assay based on water-soluble tetrazolium salts (WST-8) [41]. For genotyping, established multiplex HRM assays [24] have been further modified to determine the zygosity of 15 *G6PD* alleles. Variants identified among the studied populations, G6PD Radlowo (c.679C>T, p.Arg227Trp) and G6PD Chinese-4 + Canton (c.392G>T +c.1376G>T, p.Gly131Val+Arg459Leu), were expressed and characterised to determine their functional and structural properties compared to the corresponding single variants and the wild-type (WT) enzyme.

MATERIALS AND METHODS

Study design and participants

This retrospective study was carried out using 557 archived blood samples collected during 2019–2022 from four different

locations in Thailand: Bangkok, Kaotakiab (Prachuap Khiri Khan), Laemchabang (Chonburi) and Lopburi. The study flowchart is shown in Figure 1. Blood samples from healthy volunteers were collected and stored at −20°C until use. Under this storage condition, the integrity of samples for G6PD deficiency screening was maintained [42]. The study was approved by the Human Ethics Committee of the Faculty of Tropical Medicine, Mahidol University (approval number MUTM 2021-075-02). The participants provided written consent to have their specimens used in the research. The data were fully anonymised, and the authors had no access to information that could identify individual participants.

Phenotypic screening of G6PD deficiency by WST-8 assay

G6PD activity in 557 blood samples was measured using the WST-8 assay [41]. Blood sample (2 μL) was mixed with the reaction mixture containing 20 mM Tris–HCl pH 8.0, 10 mM $MgCl_2$, 500 μM glucose-6-phosphate (G6P), 100 μM $NADP^+$ and 100 μM WST-8 (Sigma-Aldrich, Darmstadt, Germany). The reaction was monitored by measuring the absorbance at 450 nm for 10 min using a microplate reader (Sunrise; Tecan, Männedorf, Switzerland). Haemoglobin concentration was measured using Drabkin's reagent (Sigma-Aldrich), following the manufacturer's instructions. G6PD activity was expressed as units per gram of haemoglobin (U/g Hb).

The adjusted male median (AMM) was determined and defined as 100% enzyme activity [43]. According to the World Health Organization (WHO) guidelines for phenotypic categorisation of G6PD deficiency and safe cut-off points for administering antimalarial treatments such as primaquine and tafenoquine, 30% and 70% thresholds were used [14, 44]. Samples exhibiting less than 30% enzyme activity were classified as deficient, those with enzyme activity ranging from 30% to 70% were classified as intermediate deficiency, and samples with enzyme activity exceeding 70% were classified as G6PD normal.

Development of HRM assays for detection of *G6PD* mutations and zygosity identification

Genomic DNA was extracted from blood samples using the QIAamp DNA Blood Mini Kits (QIAGEN, Hilden, Germany), following the manufacturer's instructions. DNA concentration was measured using a NanoDrop 2000 spectrophotometer (Thermo Fisher Scientific, Waltham, MA, USA).

Fifteen *G6PD* mutations common in Thailand and Southeast Asia were included in this study. To enable identification of zygosity in the *G6PD* gene, two distinct sets of primers were used: one designed for the mutant allele and another for the WT allele. In the previous study, multiplex HRM assays were developed to detect 15 *G6PD* mutations [24]. In this study, allele-specific primers were further designed for the WT. These primers were meticulously designed to generate PCR amplicons of distinct melting temperatures, allowing detection of 15 *G6PD* alleles in four reactions. The reaction conditions were optimised to prevent cross-reactions while ensuring high accuracy in detection.

HRM reaction mixture contained 6.25 μL of 2× HRM Type-It mix (QIAGEN), varying concentrations of primers, molecular-grade water and 2.5 μL of the gDNA template (2–10 ng). PCR amplification and melting curve analysis were performed on a Rotor-Gene Q instrument (QIAGEN). DNA samples with known *G6PD* genotypes (confirmed by DNA sequencing) were included in every run as WT and mutation controls. Data analysis was performed using Rotor-Gene Q software. Primers and conditions for HRM assays are listed in Tables 1 and 2.

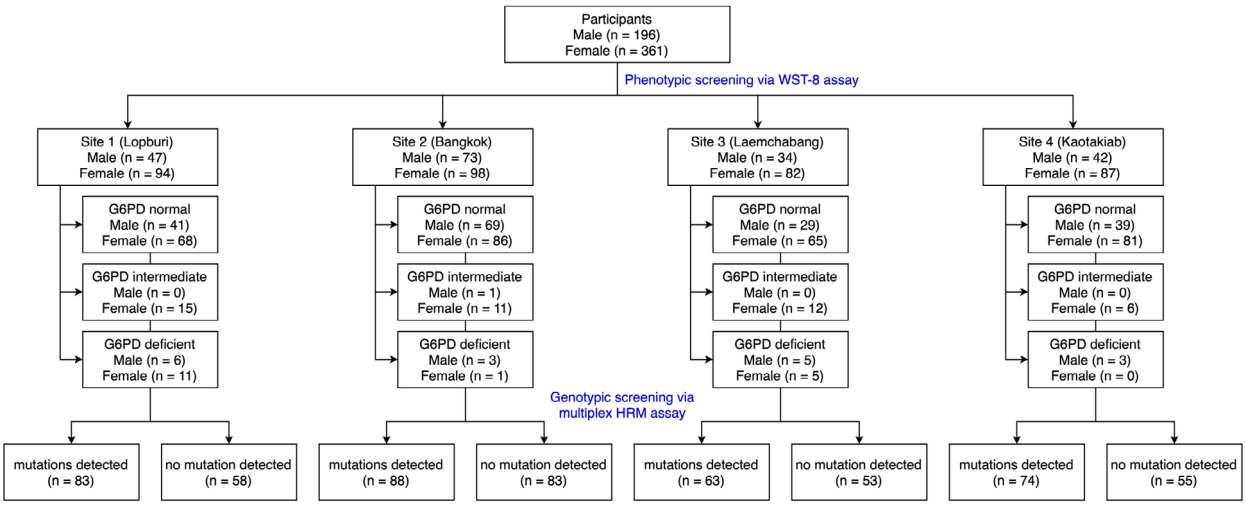

FIGURE 1 Study workflow.

TABLE 1 Primers and reaction conditions used in HRM assays for detection of WT allele.

Reaction	Primer	Primer sequence (from 5′ to 3′)	Primer concentration (nM)	T_m of PCR amplicon (°C)	T_a of PCR condition (°C)	Product size (bp)
1	A95_WF	TTC CAT CAG TCG GAT ACA CA	1500	81.3 ± 0.3	58	126
	A95_WR	CCT GCA ACA ATT AGT TGG AAA				
	G487_WF	TCC GGG CTC CCA GCA GAG	100	87.0 ± 0.3		185
	G487_WR	TTG GCC CCA CCT CAG CAC CA				
	G871_WF	GGC TTT CTC TCA GGT CAA GG	800	78.6 ± 0.3		66
	G871_WR	CCC AGG ACC ACA TTG TTG GC				
	G1376_WF	CCT CAG CGA CGA GCT CCG	600	84.1 ± 0.3		99
	G1376_WR	CTG CCA TAA ATA TAG GGG ATG G				
2	T143_WF	GAC CTG GCC AAG AAG AAG AT	600	88.4 ± 0.3	63	152
	T143_WR	CCG GCC ATC CCG GAA CAG CC				
	G392_WF	CAT GAA TGC CCT CCA CCT GG	200	85.5 ± 0.3		87
	G392_WF	TTC TTG GTG ACG GCC TCG TA				
	C563_WF	CGG CTG TCC AAC CAC ATC TC	600	80.8 ± 0.3		67
	C563_WR	CCA GGT AGT GGT CGA TGC GGT A				
	C1024_WF	CAC TTT TGC AGC CGT CGT CT	400	83.4 ± 0.3		99
	C1024_WR	CAC ACA GGG CAT GCC CAG TT				
3	T196_WF	CCT TCT GCC CGA AAA CAC CT	400	83.6 ± 0.3	63	84
	T196_WR	AAG GGC TCA CTC TGT TTG CG				
	C406_WF	CCT GGG GTC ACA GGC CAA CC	200	85.6 ± 0.3		115
	C406_WR	CAA CGG CAA GCC TTA CAT CTG GC				
	C592_WF	CCG TGA GGA CCA GAT CTA CC	800	81.2 ± 0.3		69
	C592_WR	AGC ACC ATG AGG TTC TGC ACC				
	C1360_WF	GAG CCA GAT GCA CTT CGT GC	800	87.5 ± 0.3		127
	C1360_WR	GAG GGG ACA TAG TAT GGC TT				
4	C1311_WF	CGT GAA GCT CCC TGA CGC CTA C	800	86.5 ± 0.3	63	93
	C1311_WR	CCG GCA GCT GGG CCT CAC				
	T1365-13 _WF	CCG GCC TCC CAA GCC ATA CTA T	100	83.5 ± 0.3		87
	T1365-13 _WR	CTC AAT CTG GTG CAG CAG TGG				
	486-34del_WF	CCT CAC TCC CCG AAG AGG GGT T	600	88.4 ± 0.3		339
	486-34del _WR	GGC CAC ATG TGA GGG GTC ACC				

Note: PCR amplification was carried out under the following conditions: one cycle at 95°C for 5 min, followed by 30 cycles at 95°C for 10 s, annealing for 30 s and 72°C for 10 s. HRM analysis was carried out by melting from 70 to 90°C.

The performance of the developed HRM assays was assessed. The number of true positives (TP), true negatives (TN), false positives (FP) and false negatives (FN) was determined using Sanger sequencing as the reference method. For DNA sequencing, the *G6PD* gene was amplified using previously described conditions [23]. Following amplification, PCR products were subjected to purification and sequenced (1st BASE, Apical Scientific, Malaysia).

A total of 230 DNA samples (150 G6PD-mutant and 80 G6PD-WT) were used to assess the specificity and sensitivity of the assay. Sensitivity was calculated as TP/ (TP + FN), and specificity as TN/ (FP + TN).

The developed HRM assays were then applied to detect mutations and identify zygosity of the *G6PD* gene in 557 samples. Additionally, 20 samples with a deficient or intermediate phenotype, carrying intronic or synonymous mutations or showing no detectable mutations by HRM assays, were further analysed by DNA sequencing.

Biochemical and structural characterisation of G6PD variants

Two previously uncharacterised *G6PD* mutations, *G6PD* Radlowo (identified through DNA sequencing) and *G6PD* Chinese-4 + Canton, were analysed to determine their impact on G6PD protein structure and function. The mutations were created by site-directed mutagenesis, expressed in BL21 (DE3) cells, and subsequently purified using affinity chromatography, following previous protocols [39].

TABLE 2 Primers and reaction conditions used in HRM assays for detection of mutant allele [24].

Reaction	Primer	G6PD variant	Primer sequence (from 5′ to 3′)	Primer concentration (nM)	T_m of PCR amplicon (°C)	Product size (bp)
1	A95G_MF	Gaohe	TTC CAT CAG TCG GAT ACA CG	600	80.8 ± 0.3	100
	A95G_MR		AGG CAT GGA GCA GGC ACT TC			
	G487A_MF	Mahidol	TCC GGG CTC CCA GCA GAA	400	84.5 ± 0.3	87
	G487A_MR		GGT TGG ACA GCC GGT CA			
	G871A_MF	Viangchan	GGC TTT CTC TCA GGT CAA GA	600	77.9 ± 0.3	66
	G871A_MR		CCC AGG ACC ACA TTG TTG GC			
	G1376T_MF	Canton	CCT CAG CGA CGA GCT CCT	600	83.2 ± 0.3	99
	G1376T_MR		CTG CCA TAA ATA TAG GGG ATG G			
2	T143C_MF	Aures	GAC CTG GCC AAG AAG AAG AC	400	88.4 ± 0.3	152
	T143C_MR		CCG GCC ATC CCG GAA CAG CC			
	G392T_MF	Chinese-4	CAT GAA TGC CCT CCA CCT GT	200	85.5 ± 0.3	87
	G392T_MF		TTC TTG GTG ACG GCC TCG TA			
	C563T_MF	Mediterranean	CGG CTG TCC AAC CAC ATC TT	400	82.4 ± 0.3	87
	C563T_MR		GTT CTG CAC CAT CTC CTT GC			
	C1024T_MF	Chinese-5	CAC TTT TGC AGC CGT CGT CT	400	83.4 ± 0.3	99
	C1024T_MR		CAC ACA GGG CAT GCC CAG TT			
3	T196A_MF	Songklanagarind	CCT TCT GCC CGA AAA CAC CA	400	83.8 ± 0.3	84
	T196A_MR		AAG GGC TCA CTC TGT TTG CG			
	C406T_MF	Valladolid	CCT GGG GTC ACA GGC CAA CT	400	84.6 ± 0.3	93
	C406T_MR		CTC ATG CAG GAC TCG TGA AT			
	C592T_MF	Coimbra	CCG TGA GGA CCA GAT CTA CT	400	81.9 ± 0.3	78
	C592T_MR		CCC CAC CTC AGC ACC ATG			
	C1360T_MF	Union	GAG CCA GAT GCA CTT CGT GT	200	87.9 ± 0.3	127
	C1360T_MR		GAG GGG ACA TAG TAT GGC TT			
4	C1311T_MF		CGT GAA GCT CCC TGA CGC CTA T	800	85.2 ± 0.3	93
	C1311T_MR		CCG GCA GCT GGG CCT CAC			
	T1365-13C _MF		CCG GCC TCC CAA GCC ATA CC	200	83.6 ± 0.3	87
	T1365-13C _MR		CTC AAT CTG GTG CAG CAG TGG			
	486-34delT _MF		CCT CAC TCC CCG AAG AGG GGT C	400	82.3 ± 0.3	64
	486-34delT _MR		TTC CAG CCT CTG CTG GGA GC			

Note: PCR amplification was carried out under the following conditions: one cycle at 95°C for 5 min, followed by 30 cycles at 95°C for 10 s, 63°C for 30 s and 72°C for 10 s. HRM analysis was carried out by melting from 70 to 90°C.

Steady-state kinetic parameters were determined to assess the effects of mutations on the catalytic activity of G6PD variants. The enzymatic reaction was monitored by following the formation of NADPH at 340 nm using a UV–VIS spectrophotometer (Shimadzu, Kyoto, Japan). To determine the K_m for G6P, the concentration of $NADP^+$ was fixed at 100 μM while varying concentrations of G6P from 2.5 to 1000 μM and to determine the K_m for $NADP^+$, the concentration of G6P was fixed at 500 μM while varying concentrations of $NADP^+$ from 1 to 200 μM.

Various approaches were employed to assess the effect of mutations on structural stability, including thermal stability assay, thermal inactivation assay, as well as susceptibility to trypsin digestion and guanidine-hydrochloride (Gdn-HCl) treatment. These experiments were carried out according to previously published protocols [45].

X-ray crystallography unveiled the crucial structural $NADP^+$-binding site, pivotal for stabilising the G6PD protein structure [46]. Consequently, structural stability analyses were conducted under various $NADP^+$ concentrations (0, 10 and 100 μM). For thermal stability analysis, the proteins were exposed to increasing temperatures (20–80°C) in the presence of 5X SYPRO Orange reporter dye, during which protein unfolding was monitored and the temperature at which half of the protein unfolded was defined as the T_m. A protein exhibiting a higher T_m value demonstrates greater heat tolerance, suggesting greater structural stability. In thermal inactivation analysis, the proteins were incubated at different temperatures (25–65°C) for 20 min, and the

residual enzyme activity was measured. $T_{1/2}$ of each protein was determined and expressed as the temperature at which the enzyme lost 50% of its activity. A protein with a greater $T_{1/2}$ value suggests greater structural stability.

The protein structure unfolds when exposed to increasing concentrations of Gdn-HCl, allowing the determination of the structural stability of G6PD variants through the measurement of residual enzyme activity. Susceptibility to Gdn-HCl treatment was assessed by incubating G6PD proteins with different concentrations of Gdn-HCl (0–0.5 M) for 2 h. The residual enzyme activity was measured, and $C_{1/2}$ was defined as the concentration of Gdn-HCl at which the enzyme lost 50% of its activity. Susceptibility to trypsin digestion was assessed by incubating G6PD proteins with 0.5 mg/mL trypsin for 5 min, while the residual enzyme activity was measured and expressed as a percentage of the activity of the same enzyme incubated without trypsin.

Molecular dynamic simulations

The G6PD dimeric structure in complex with two G6P substrates and four $NADP^+$ ligands was prepared using molecular docking techniques according to previously published procedures [47]. The G6PD variant structures incorporating the following mutations: Arg227Trp, Gly131Val, Arg459Leu and Gly131Val + Arg459Leu were generated utilising the mutagenesis tool from the wizard menu of PyMOL software (http://www.pymol.org/pymol). The WT and variant structures were subjected to simulation using the GROMACS 2018.1 package. Protein structures were prepared using the pdb2gmx utility and GROMOS96 54a7 force field while the ligand topology files were generated from the Automated Topology Builder (ATB) server [48, 49]. The protein-ligand complex was assembled, and the system was prepared according to conditions described in previously published protocols [47]. The production run was subjected to 100 ns repeated twice for each variant. Conformational analysis at several critical regions such as the mutation site, dimer and tetramer interfaces, and protein-ligand affinities were performed by comparing the post-simulated variant structures against the WT. Structural images were generated using the PyMOL Visualizer.

RESULTS

The prevalence of G6PD deficiency

This study included 557 samples (196 males and 361 females) collected from four locations in Thailand (Figure 2). The AMM of the studied population was determined to be 10.06 ± 0.97 U/gHb. Of the 557 samples, 6.10% (17 males and 17 females) were G6PD deficient (<30% enzyme activity; 0.14–2.79 U/gHb), 8.08% (1 male and 44 females) were classified as intermediate deficiency (30%–70% enzyme activity; 3.07–6.98 U/gHb) and 85.82% (178 males and 300 females) were classified as G6PD normal (>70% enzyme activity; 7.10–17.15 U/gHb). The distribution of enzyme activity among the studied population, stratified into deficiency, intermediate deficiency and G6PD normal, is shown in Figure 3.

Development of HRM assays for detection of *G6PD* mutations and zygosity identification

HRM assays were developed to allow detection and zygosity identification of 15 *G6PD* alleles in four reactions. In mutant allele detection, the presence of mutation is indicated by a peak at the corresponding melting temperature, whereas samples without mutations had no amplification, resulting in a flat line (Figure 4). In WT allele detection, the WT sample exhibits a peak at the temperature that corresponds to its specific genotype (Figure 5). For identifying *G6PD* zygosity, hemizygote and homozygote samples display a peak at the corresponding melting temperature in primer sets targeting the mutation allele, while exhibiting no peak in primer sets targeting the WT allele (Figure 6). Heterozygote samples show peaks at the corresponding melting temperatures in both mutation and WT primer sets. For validation, DNA sequencing was employed as the reference method. The developed HRM assays demonstrated a sensitivity (confidence interval [CI]: 97.47%–100%) and specificity (CI: 95.49%–100%) of 100% in detecting 15 *G6PD* mutations and determining zygosity.

G6PD genotypes and allele frequency

Out of the 557 samples examined, 308 samples (79 males and 229 females) were found to carry a spectrum of *G6PD* mutations, including 11 missense, one synonymous and two intronic mutations (Table 3). The HRM assays revealed various *G6PD* genotypes, among which was a double missense mutation (*G6PD* Chinese-4 + Canton; c.392G>T and c.1376G>T), contributing to the deficient phenotype.

Among the 20 samples analysed by DNA sequencing, 14 showed results consistent with HRM assays. Of these, 10 samples carried the c.1311C>T and c.1365-13T>C mutations, while another four carried the c.486-34delT mutation. Notably, six samples were found to carry mutations not included in HRM assay panels. Among them, a female with an intermediate activity of 5.91 U/gHb was found to carry compound mutations (c.679C>T, c.1311C>T and c.1365-13T>C). The mutation c.679C>T was identified as *G6PD* Radlowo, marking its first discovery in Thailand. Among the remaining five samples, one carried *G6PD* Orissa, along with synonymous and intronic mutations (c.131C>G, c.486-34delT, c.1311C>T and c.1365-13T>C). Two samples carried *G6PD* Kaiping (c.1388G>A), while the other two had *G6PD* Kaiping coexisting with a deletion mutation (c.1388G>A and c.486-34delT).

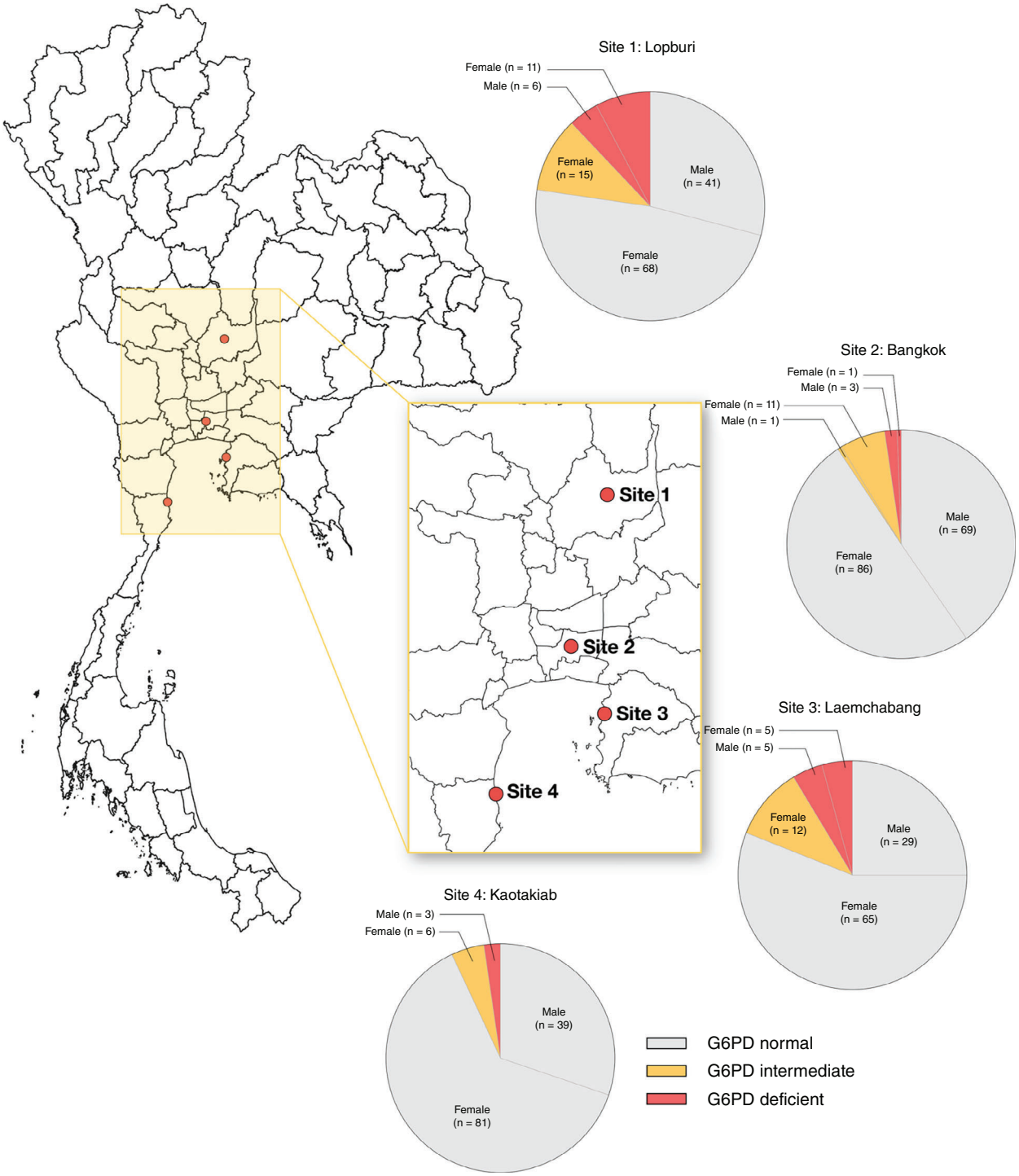

FIGURE 2 G6PD phenotype of samples across the different collection sites.

The most common *G6PD* genotype identified in the studied population was a combination of synonymous and intronic mutations (c.1311C>T and c.1365-13T>C), accounting for 57.47%. The compound mutations associated with the missense *G6PD* Viangchan variant (c.871G>A, c.1311C>T and c.1365-13T>C) were detected at a frequency of 15.26%. Additionally, the deletion in intron 5 (c.486-34delT) was found at a frequency of 10.06%. Although the *G6PD* mutations identified in this study have been previously documented, novel *G6PD* genotypes, comprising various combinations of mutations, have been discovered. These include compound mutations associated with *G6PD* Orissa (c.131C>G, c.486-34delT, c.1311C>T and c.1365-13T>C), compound mutations associated with *G6PD* Radlowo (c.679C>T, c.1311C>T and c.1365-13T>C) and a combination of missense *G6PD*

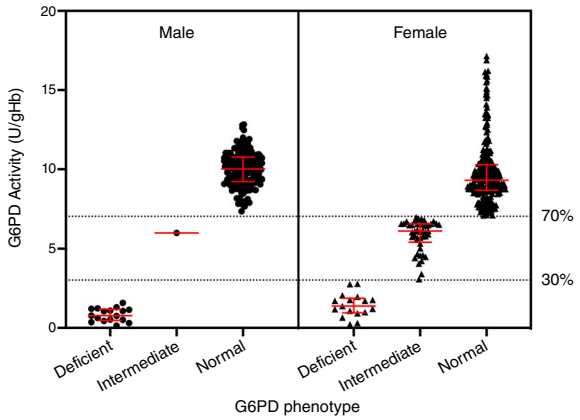

FIGURE 3 Distribution of G6PD activity among males and females, categorised into deficiency, intermediate deficiency and G6PD normal subjects.

Kaiping with deletion mutations (c.1388G>A and c.486-34delT). The distribution of *G6PD* genotypes varied across the different sample collection sites. The zygosity of all samples with *G6PD* mutations was determined.

Table 4 shows the zygosity and allele frequency of *G6PD* mutations among the studied population. The HRM assays developed in this study accurately identified all male samples as hemizygotes. Among female samples, the majority of G6PD genotypes are heterozygotes. Specifically, four samples are homozygous for c.871G>A, c.1311C>T and c.1365-13T>C, while nine samples carry a combination of heterozygous c.871G>A and homozygous c.1311C>T and c.1365-13T>C. Sixteen samples exhibit homozygosity for c.1311C>T and c.1365-13T>C, and one sample is homozygous for c.486-34delT. Geographical characteristics of G6PD deficiency and mutations are shown in Table 5.

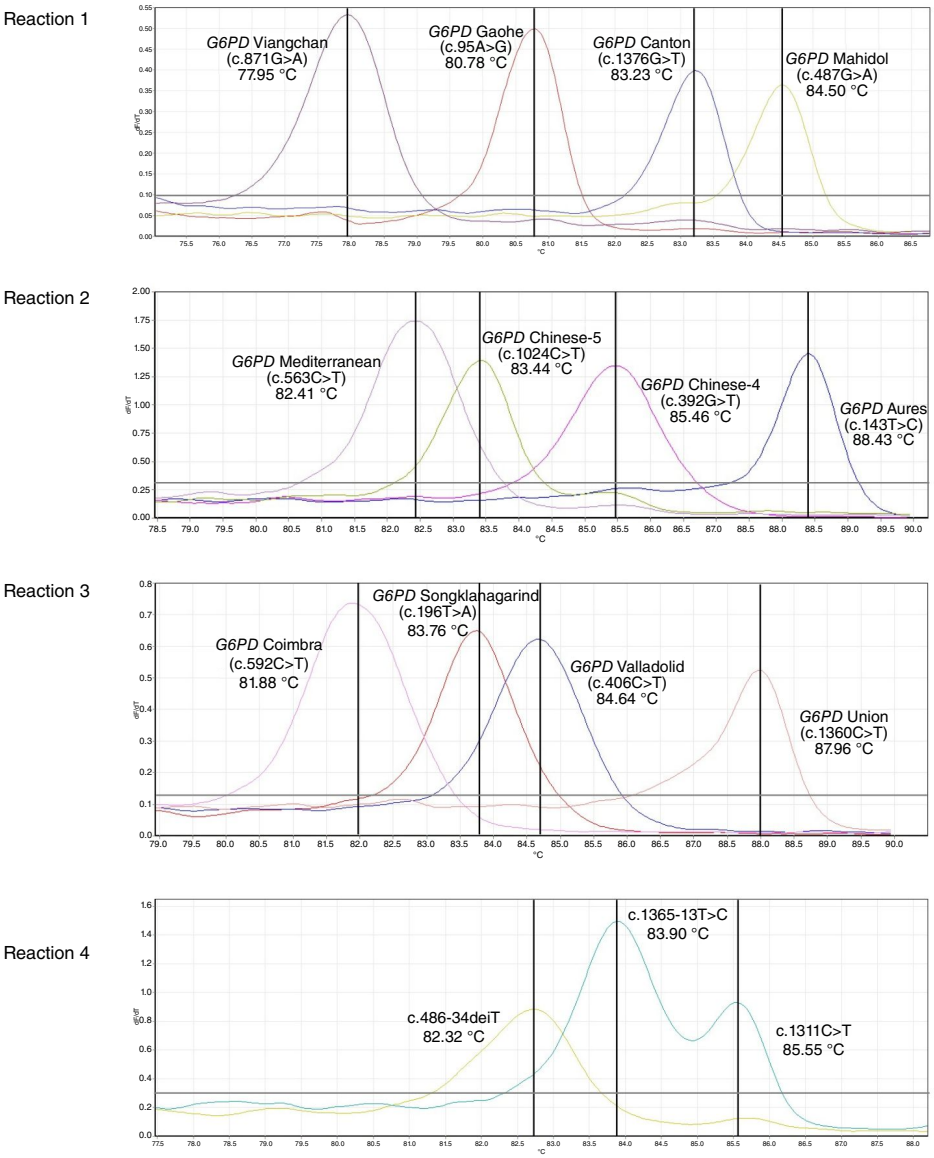

FIGURE 4 HRM reactions for identification of *G6PD* mutations.

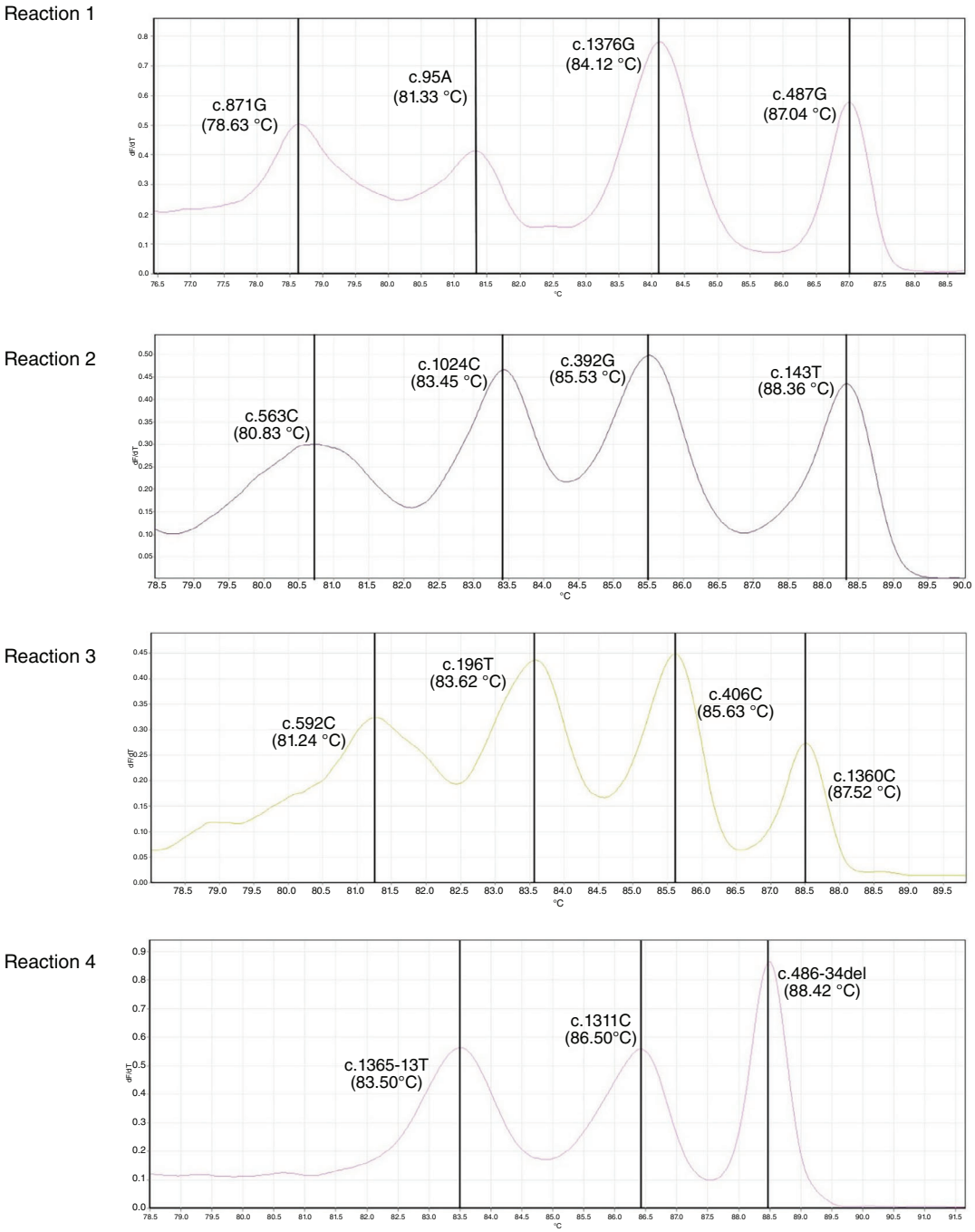

FIGURE 5 HRM reactions for identification of *G6PD* WT.

Relationship of *G6PD* genotypes and enzyme activity

Table 6 shows the G6PD activity profile in individuals with *G6PD* mutations. A wide range of G6PD activity levels was observed among individuals with *G6PD* mutations (0.14–12.61 U/gHb in males and 0.23–16.22 U/gHb in females, Figure 7). Out of the 79 males carrying *G6PD* mutations, 17 samples were G6PD-deficient (0.14–1.58 U/gHb), one had intermediate deficiency (6.00 U/gHb) and 61 samples had normal G6PD enzyme activity (7.36–12.61 U/gHb). Among 229 females with detected *G6PD* mutations, 17 samples were G6PD-deficient (0.23–2.79 U/gHb), 44 samples were of intermediate deficiency (3.07–6.98 U/gHb) and 168 samples had normal enzyme activity (7.10–16.22 U/gHb).

While nearly all missense mutations are deemed pathogenic that can cause enzyme deficiency by altering catalytic activity and/or decreasing structural stability, the precise impact of synonymous (c.1311C>T) and intronic (c.1365-13T>C and c.486-34delT) mutations remains unclear. As expected, 16 hemizygous males and one compound heterozygous female carrying missense mutations

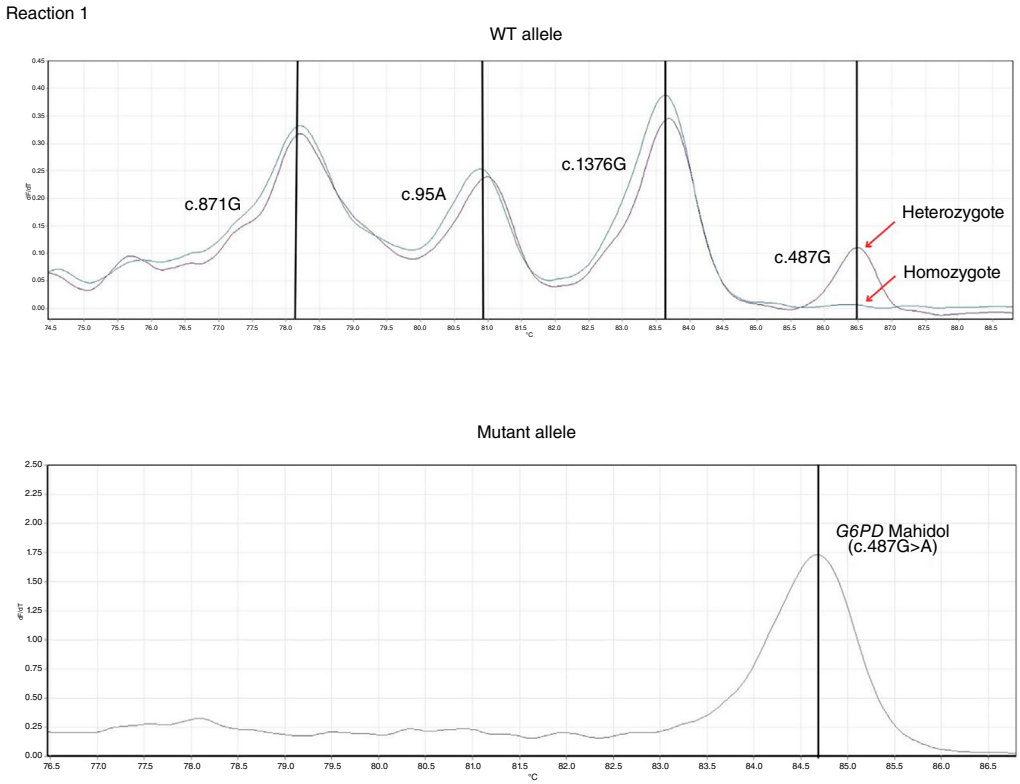

FIGURE 6 Representative HRM profiles for the identification of hemizygous/homozygous and heterozygous for *G6PD* Mahidol.

TABLE 3 *G6PD* genotypes identified in this study.

Number	Genotype	Variant name	Collection site 1	2	3	4	Total (*n*)	Frequency
1	c.131C>G*, c.486-34delT, c.1311C>T, c.1365-13T>C	Orissa	—	—	—	1	1	0.32
2	c.143T>C	Aures	1	—	—	—	1	0.32
3	c.392G>T	Chinese-4	—	—	4	—	4	1.30
4	c.392G>T, c.1311C>T, c.1365-13T>C	Chinese-4	—	—	1	—	1	0.32
5	c.392G>T, c.1376G>T	Chinese-4 Canton	—	—	1	—	1	0.32
6	c.406C>T, c.1311C>T, c.1365-13T>C	Valladolid	—	1	1	—	2	0.65
7	c.486-34delT	—	6	13	4	8	31	10.06
8	c.486-34delT, c.1311C>T, c.1365-13T>C	—	2	4	2	3	11	3.57
9	c.487G>A	Mahidol	3	1	1	2	7	2.27
10	c.487G>A, c.486-34delT	Mahidol	1	—	—	—	1	0.32
11	c.679C>T*, c.1311C>T, c.1365-13T>C	Radlowo	—	1	—	—	1	0.32
12	c.871G>A, c.1311C>T, c.1365-13T>C	Viangchan	15	13	14	5	47	15.26
13	c.871G>A, c.486-34delT, c.1311C>T, c.1365-13T>C	Viangchan	1	2	—	—	3	0.97
14	c.1024C>T	Chinese-5	1	—	—	—	1	0.32
15	c.1311C>T, c.1365-13T>C	—	49	46	30	52	177	57.47
16	c.1365-13T>C	—	2	5	—	2	9	2.92
17	c.1376G>T	Canton	1	2	2	1	6	1.95
18	c.1388G>A*	Kaiping	1	—	1	—	2	0.65
19	c.1388G>A*, c.486-34delT	Kaiping	—	2	—	—	2	0.65
Total			83	90	61	74	308	100

Note: The asterisk indicates *G6PD* genotypes identified by DNA sequencing.

TABLE 4 Zygosity and allele frequency of *G6PD* mutations.

Genotype	Hemizygous male (X*Y)	Homozygous female (X*X*)	Heterozygous female (X*X)	Allele frequency
c.131C>G*	—	—	1	0.001
c.143T>C	—	—	1	0.001
c.392G>T	2	—	4	0.004
c.406C>T	—	—	2	0.001
c.486-34delT	11	2	37	0.037
c.487G>A	2	—	6	0.006
c.679C>T*	—	—	1	0.001
c.871G>A	9	8	37	0.040
c.1024C>T	—	—	1	0.001
c.1311C>T	59	78	145	0.209
c.1365-13T>C	61	78	152	0.215
c.1376G>T	3	—	4	0.005
c.1388G>A*	—	—	4	0.003

Note: The asterisk indicates *G6PD* genotypes identified by DNA sequencing.

TABLE 5 Geographical characteristics of G6PD deficiency and mutations.

			Phenotype (*n*)						Genotype (*n*)			
	Participants (*n*)		Normal		Intermediate		Deficient		Mutation detected		No mutation detected	
Sample collection site	M	F	M	F	M	F	M	F	M	F	M	F
Site 1: Lopburi	47	94	41	68	—	15	6	11	23	60	24	34
Site 2: Bangkok	73	98	69	86	1	11	3	1	23	65	50	33
Site 3: Laemchabang	34	82	29	65	—	12	5	5	12	51	22	31
Site 4: Kaotakiab	42	87	39	81	—	6	3	-	21	53	21	34
Total	196	361	178	300	1	44	17	17	79	229	117	132

TABLE 6 G6PD activity profile in individuals with *G6PD* mutations.

	Male			Female		
G6PD genotypes	Deficiency ($n = 17$)	Intermediate deficiency ($n = 1$)	Normal G6PD activity ($n = 61$)	Deficiency ($n = 17$)	Intermediate deficiency ($n = 44$)	Normal G6PD activity ($n = 168$)
Missense mutations	16 (0.14–1.58 U/gHb)	—	—	14 (0.23–2.05 U/gHb)	34 (3.40–6.89 U/gHb)	16 (7.10–8.83 U/gHb)
c.486-34delT	—	—	11 (7.67–12.61 U/gHb)	1 (2.76 U/gHb)	—	19 (7.28–12.95 U/gHb)
c.1311C > T and c.1365-13 T > C	1 (1.21 U/gHb)	1 (6.00 U/gHb)	48 (7.36–11.56 U/gHb)	2 (1.97–2.79 U/gHb)	8 (5.75–6.98 U/gHb)	117 (7.24–16.22 U/gHb)
c.1365-13 T > C	—	—	2 (8.73–10.16 U/gHb)	—	2 (3.07–6.16 U/gHb)	5 (7.82–13.41 U/gHb)
c.486-34delT, c.1311C > T and c.1365-13 T > C	—	—	—	—	—	11 (7.39–13.25 U/gHb)

showed deficient enzyme activity (male: 0.14–1.58 U/gHb and female: 1.08 U/gHb). Due to random X-inactivation, heterozygous females carrying missense mutations exhibited a broad spectrum of enzyme activity, ranging from deficient levels (13 samples; 0.23–2.05 U/gHb) to intermediate levels (34 samples; 3.40–6.89 U/gHb) and normal levels (16 samples; 7.10–8.83 U/gHb).

Remarkably, synonymous and intronic mutations can result in diverse phenotypes (deficiency, intermediate deficiency and normal) in both males and females. The deletion c.486-34delT mutation was observed in 1 female with a deficient phenotype and in 11 males and 19 females with normal G6PD enzyme activity. The combination of c.1311C>T and c.1365-13T>C mutations was detected in three G6PD-

deficient samples (one male and two females), nine samples with intermediate deficiency (one male and eight females) and 165 samples (48 males and 117 females) with normal enzyme activity. The intronic mutation c.1365-13T>C was found in two females exhibiting intermediate deficiency and in seven samples with normal G6PD enzyme activity (two males and five females). The compound mutations (c.486-34delT, c.1311C>T and c.1365-13T>C) were detected in 11 females exhibiting normal G6PD activity.

Biochemical and structural characterisation of G6PD variants

Steady-state kinetic parameters were determined to evaluate the impact of G6PD mutations on the enzyme's catalytic activity (Table 7). The binding affinity for the $NADP^+$ substrate remained unaffected by any G6PD variants studied. However, the binding affinity for the G6P substrate was found to increase in the G6PD Radlowo and G6PD Canton variants. Regarding catalytic activity, G6PD Chinese-4 exhibited a moderate impact, being the least affected variant, followed by G6PD Canton and G6PD Radlowo, which caused decreases in catalytic activity of approximately 2-fold, 6-fold and 22-fold, respectively, compared to the WT enzyme. The combined effect of single mutations was observed in the double variant, G6PD Chinese-4 + Canton, resulting in a reduction of approximately 12-fold.

The impact of mutations on structural stability was evaluated in terms of thermal stability as well as susceptibility to chemical denaturant and trypsin digestion. Structural stability analyses suggested that each G6PD mutation contributed differently to structural stability, with G6PD Chinese-4 being the least affected variant, followed by G6PD Canton, G6PD Chinese-4 + Canton and G6PD Radlowo (Table 8 and Figure 8). Notably, G6PD Radlowo remarkably destabilised the protein structure, as evidenced by markedly lower T_m (43.2°C) and $T_{1/2}$ (32.0°C) values compared to those of the WT enzyme ($T_m = 51.7$°C and $T_{1/2} = 49.8$°C). The combined effect of Chinese-4 and Canton mutations was observed in the double variant, having lower T_m (46.2°C) and $T_{1/2}$ (36.8°C) values compared to those of the single mutations: G6PD Chinese-4 ($T_m = 48.2$°C and $T_{1/2} = 45.3$°C) and G6PD Canton ($T_m = 48.1$°C and $T_{1/2} = 43.6$°C). In terms of susceptibility to chemical denaturation and trypsin digestion, the WT enzyme retained 50% of its activity at 0.18 M of Gdn-HCl and showed approximately 10% residual activity during trypsin digestion. G6PD Chinese-4, G6PD Canton and G6PD Chinese-4 + Canton showed $C_{1/2}$ values of 0.1, 0.07 and 0.06 M, respectively. G6PD Radlowo proved to be the least stable variant, exhibiting the highest susceptibility to both Gdn-HCl treatment ($C_{1/2} = 0.03$ M) and trypsin

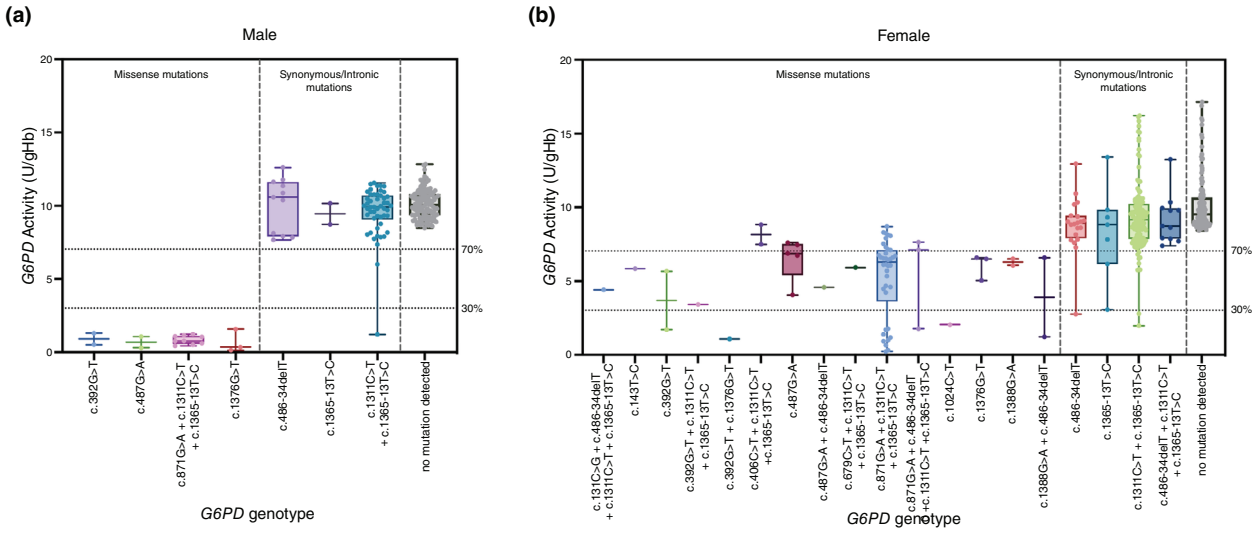

FIGURE 7 Distribution of G6PD activity by mutation types in (a) male and (b) female subjects.

TABLE 7 Kinetic parameters of recombinant G6PD variants.

Construct	Amino acid change	k_{cat} (s^{-1})	K_m G6P (μM)	K_m $NADP^+$ (μM)
WT	—	354.6 ± 23.5	47.3 ± 3.5	8.3 ± 2.2
Radlowo	Arg227Trp	15.9 ± 0.8	35.5 ± 6.0	10.7 ± 2.2
Chinese-4	Gly131Val	164.7 ± 6.7	46.8 ± 5.0	7.4 ± 1.2
Canton	Arg459Leu	61.7 ± 3.9	25.4 ± 3.3	10.1 ± 2.4
Chinese-4 + Canton	Gly131Val + Arg459Leu	30.1 ± 3.8	45.2 ± 10.3	8.2 ± 2.2

TABLE 8 Structural stability analyses of G6PD variants.

Variant	T_m (°C)			$T_{1/2}$ (°C)			$C_{1/2}$ (M)			% residual activity		
	0 μM $NADP^+$	10 μM $NADP^+$	100 μM $NADP^+$	0 μM $NADP^+$	10 μM $NADP^+$	100 μM $NADP^+$	0 μM $NADP^+$	10 μM $NADP^+$	100 μM $NADP^+$	0 μM $NADP^+$	10 μM $NADP^+$	100 μM $NADP^+$
WT	51.7 ± 0.0	55.6 ± 0.0	59.0 ± 0.0	49.8 ± 0.5	54.9 ± 0.2	59.3 ± 0.1	0.2 ± 0.0	0.3 ± 0.0	0.4 ± 0.0	9.7 ± 2.3	68.6 ± 5.0	88.0 ± 5.8
Radlowo	43.2 ± 0.0	46.9 ± 0.0	47.9 ± 0.0	32.0 ± 0.8	49.8 ± 0.1	55.0 ± 0.5	0.0 ± 0.0	0.0 ± 0.0	0.1 ± 0.0	2.0 ± 0.3	60.9 ± 0.7	79.3 ± 0.7
Chinese-4	48.2 ± 0.0	52.4 ± 0.0	55.6 ± 0.0	45.3 ± 0.1	52.3 ± 0.5	56.4 ± 1.0	0.1 ± 0.0	0.2 ± 0.0	0.3 ± 0.0	2.8 ± 0.4	54.2 ± 1.7	77.1 ± 3.0
Canton	48.1 ± 0.0	50.8 ± 0.0	53.3 ± 0.0	43.6 ± 0.6	50.1 ± 0.0	53.3 ± 0.0	0.1 ± 0.0	0.2 ± 0.0	0.2 ± 0.0	2.2 ± 0.5	19.3 ± 1.4	31.6 ± 1.4
Chinese-4 + Canton	46.2 ± 0.0	47.6 ± 0.0	49.2 ± 0.0	36.8 ± 0.4	46.5 ± 1.0	49.2 ± 0.3	0.1 ± 0.0	0.1 ± 0.0	0.1 ± 0.0	3.5 ± 0.6	40.4 ± 2.8	57.0 ± 6.5

Note: Thermal stability assay: T_m was defined as the temperature at which half of the protein unfolded and expressed as mean ± SD. Thermal inactivity assay: $T_{1/2}$ was defined as the temperature at which the enzyme lost 50% of its activity and expressed as mean ± SE. Susceptibility to Gdn-HCl treatment: $C_{1/2}$ was defined as the concentration of Gdn-HCl at which the enzyme lost 50% of its activity and expressed as mean ± SE. Trypsin digestion: The residual enzyme activity was expressed as a percentage of the activity of the same enzyme incubated without trypsin and expressed as mean ± SE.

digestion, resulting in residual activity as low as 2%. The presence of $NADP^+$ was found to improve structural stability in a concentration-dependent manner across all structural stability tests, underscoring its pivotal role in stabilising the G6PD protein structure.

Structural analysis of G6PD variants by molecular dynamics simulations

Molecular dynamic simulations were utilised to investigate mutation-induced structural changes within crucial regions of the G6PD dimer structure, such as the G6P substrate and $NADP^+$ binding sites, along with the dimer and tetramer interfaces (Figure 9). Conformational alterations at the mutation sites were analysed and presented in Table 9 and Figure 10. Since the activity of the G6PD enzyme relies on its existence in either dimer or tetramer states, the integrity of the interfaces between these structures is vital for both the enzyme's functionality and stability [45]. Hence, the dimer and tetramer interfaces were evaluated by determining the presence of hydrogen bonds between the βN-βN strands and salt bridges between the monomeric subunit of the dimer, as well as computing the surface area of the residues responsible for establishing salt bridges at the tetramer interface for the WT and variants (Table 10). The G6PD Radlowo variant, located near critical enzyme function regions such as the structural $NADP^+$ binding site, the dimer and tetramer interfaces, displayed significant structural changes affecting its activity and stability. Substitution at residue 227 disrupted interactions with neighbouring residues, possibly attributed to the high flexibility observed in the αg-βG and βI-βJ loops (Figure 10a). This mutation also affected dimerization and increased solvent accessibility at the tetramer interface, indicated by an increased SASA value (Figure 11a and Table 10). Despite favouring the tetrameric state, this variant failed to retain the Lys171-catalytic $NADP^+$ hydrogen bond (Figure 12).

The replacement of a positively charged arginine with a hydrophobic leucine in G6PD Canton disrupts the structure's ability to maintain interhelical interactions between αe (177–190) and αn (455–473). This mutation located close to the dimer interface and the structural $NADP^+$ binding site hinders the formation of dimer salt bridges and hydrogen bonds between βN-βN strands reflected by high βN-βN distance (Figure 11c), resulting in dissociated monomeric subunits and loosely packed protein structure. While maintaining the Lys171-G6P hydrogen bond, it exhibited lower affinity for catalytic $NADP^+$ (Figure 12). G6PD Chinese-4 mutation slightly alters the positioning of βE-αe loop in the G6PD enzyme, leading to a minor enhancement in its affinity for catalytic $NADP^+$ (Figure 10b). Despite this change, it retains crucial interactions at the dimer interface and exhibits high integrity as a dimeric enzyme (Figure 11b). Additionally, Lys 171 residue retains hydrogen bonds with both G6P and catalytic $NADP^+$, resulting in higher enzyme activity

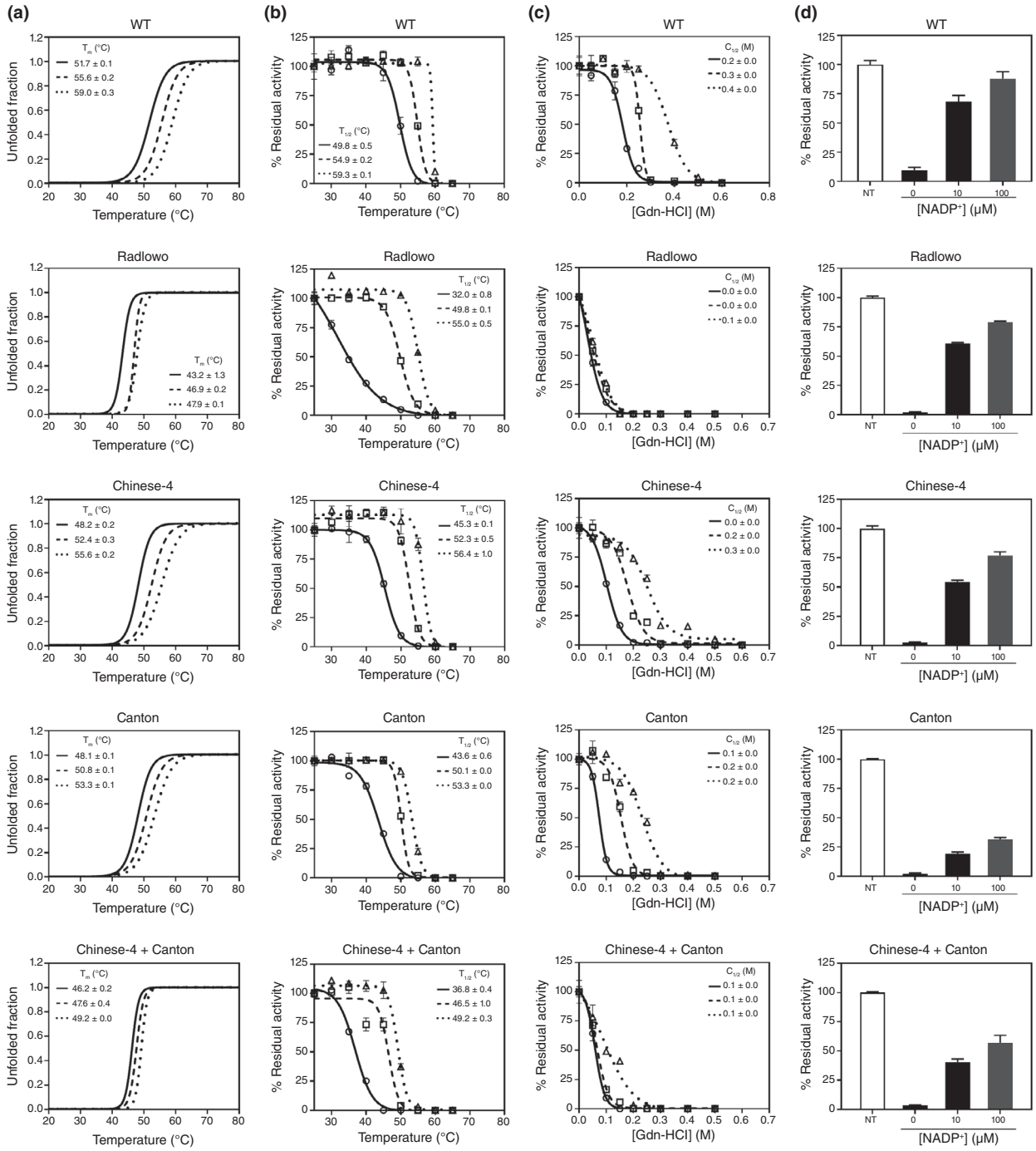

FIGURE 8 Structural stability analyses of G6PD variants. The effect of mutations was assessed in the absence (solid line) and presence of $NADP^+$ (10 μM: Dashed line and 100 μM: Dotted line). (a) Thermal stability assay. T_m was defined as the temperature at which half of the protein unfolded and presented as mean ± SD of triplicate measurements. (b) Thermal inactivation analysis. $T_{1/2}$ was defined as the temperature at which the enzyme lost 50% of its activity and presented as mean ± SE of triplicate measurements. (c) Susceptibility to Gdn-HCl treatment. $C_{1/2}$ was defined as the concentration of Gdn-HCl at which the enzyme lost 50% of its activity and presented as mean ± SE of triplicate measurements. (d) Susceptibility to trypsin digestion. NT: No trypsin treatment. Error bars represent the mean ± SE of triplicate measurements.

compared to other variants (Figure 12). Interestingly, this mutation did not significantly affect the enzyme's overall structure as it is located away from ligand binding sites, dimer and tetramer interfaces. The corresponding double variant, G6PD Chinese-4 + Canton exhibits increased displacement between mutated residues and their neighbours compared to single variants (Table 9), resulting in reduced enzyme activity due to impaired dimerization characterised by loss of key hydrogen bonds and increased distance between βN–βN strands (Figure 11d). Despite these structural alterations, affinities for G6P and catalytic $NADP^+$ remain unaffected, as determined by Lys 171-G6P and Lys

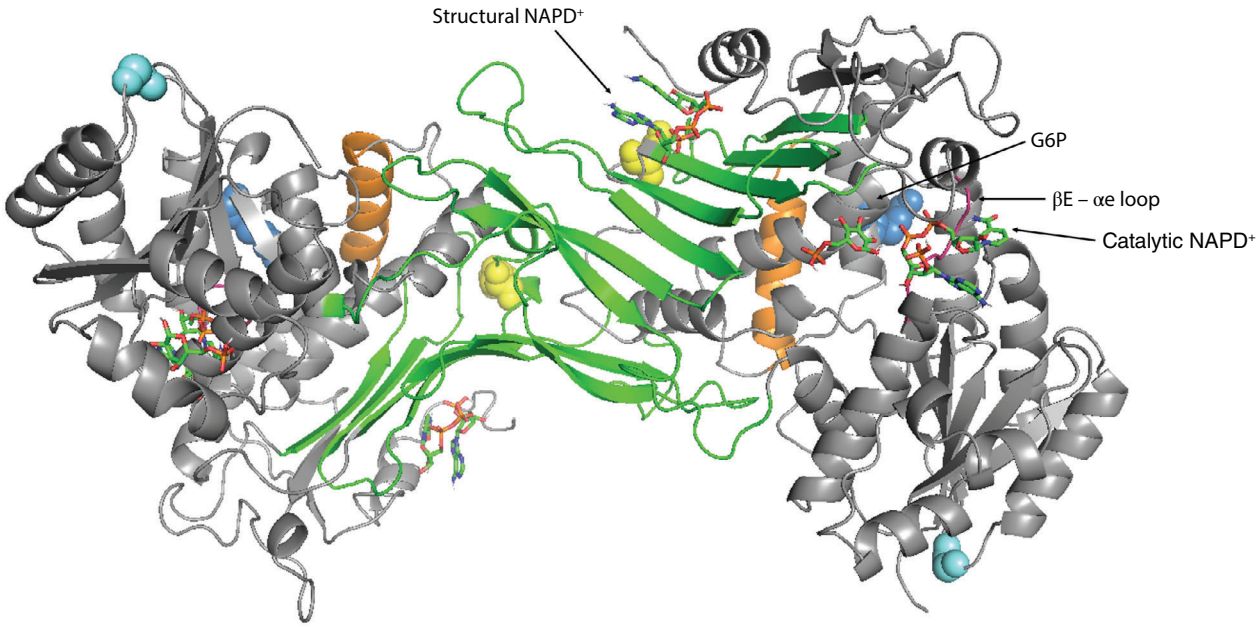

FIGURE 9 Cartoon view of G6PD dimer highlighting the mutation location in spheres (G6PD Radlowo; yellow, G6PD Chinese-4; cyan, G6PD Canton; blue), important domains—dimer interface (green), tetramer interface (orange), catalytic βE—αe loop (red) and ligand binding sites.

TABLE 9 Distance between the mutation site and neighbouring residues for the WT and variants.

Mutation site			Distance (Å)		
Variant	**Position**	**Mutated residue**	**Neighbouring residue**	**WT**	**Variant**
Radlowo	227	Arg > Trp (αg-βG loop 223–231)	Asp350 (βI-βJ loop 343–353)	3.3	6.8
Chinese-4	131	Gly > Val (αc-βD loop 129–134)	Arg 136 (βD 135–140)	2.9	3.3
Canton	459	Arg > Leu (αn 455–473)	Asp 181 (αe 177–190)	2.6	3.7
Chinese-4 + Canton	131	Gly > Val (αc-βD loop 129–134)	Arg 136 (βD 135–140)	2.9	3.1
	459	Arg > Leu (αn 455–473)	Asp 181 (αe 177–190)	2.6	4.0

171-catalytic $NADP^+$ hydrogen bond formations at ligand binding sites (Figure 12).

DISCUSSION

The primary clinical concern associated with G6PD deficiency is haemolytic anaemia, triggered by exposure to certain triggers, such as certain foods, infections or medications (e.g., antimalarial drugs such as primaquine and tafenoquine) [50–52]. In Thailand, access to healthcare services may vary across regions. Routine screening of G6PD deficiency is not practiced, but it is performed in response to adverse events such as newborn jaundice or drug-induced haemolysis. Thus, ensuring accurate diagnosis of G6PD deficiency is vital to prevent adverse reactions to medications. Comprehensive knowledge of the prevalence and distribution of G6PD deficiency in the population is particularly important as it informs malaria treatment strategies, including the use of antimalarial drugs and strategies for preventing transmission.

Phenotypic tests for G6PD deficiency, while widely used, may not always provide sufficient information. This is because enzyme activity levels can be influenced by several variables, including the age of red blood cells, age and sex of the individuals, recent blood transfusions, medications and concurrent illnesses, among others [6]. In these instances, misclassification may give rise to clinical complications. Moreover, an appreciable number of newborns with intermediate G6PD activity experienced severe hyperbilirubinaemia needing phototherapy [15, 53].

In addition, certain *G6PD* variants with mild deficiency may exhibit normal enzyme activity levels under baseline conditions but can become deficient under oxidative stress, which is not adequately captured in phenotypic tests. For example, Mahidol (c.487G>A), and A^- (c.376A>G +c.202G>A or c.376A>G+c.968C>T) variants may present with normal enzyme activity levels in routine phenotypic tests but can lead to haemolysis under certain conditions [23, 54, 55]. Furthermore, random X-inactivation could also lead to variations in enzyme activity levels among individuals, making phenotypic testing less reliable. Phenotypic

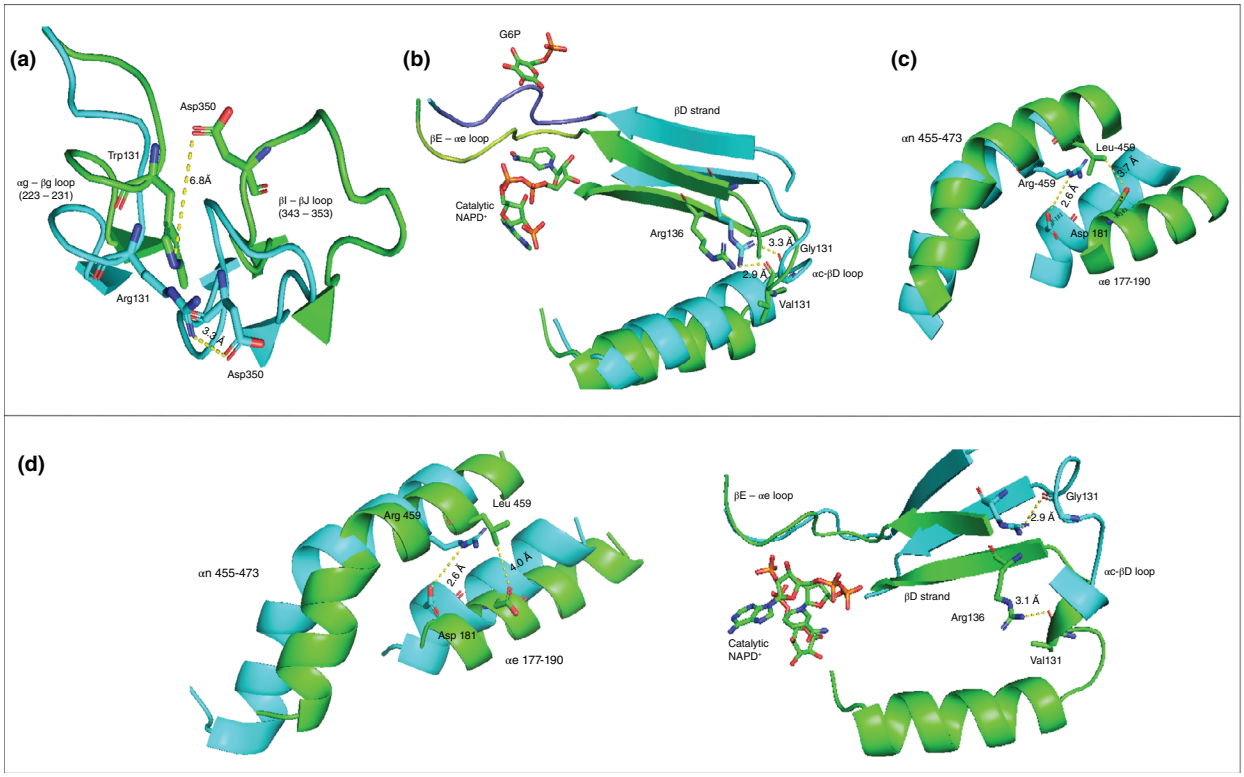

FIGURE 10 Alterations in the intermolecular interactions due to mutation in the variant structures (green) in comparison to WT (cyan). (a) G6PD Radlowo, (b) G6PD Chinese-4, (c) G6PD Canton and d) G6PD Chinese-4 + Canton double variant showing changes at the R459L mutation site (left) and G131V mutation site (right).

TABLE 10 Structural characteristics of the dimer and tetramer interfaces for the WT and variants.

	Dimer					Tetramer
	βN–βN H-bonds		βN–βN distance (A)	Salt bridges at the dimer interface		SASA of tetramer salt bridge residues (nm^2)
G6PD	Asp 421–asp 421	Glu 419–Thr 423		Glu 206–Lys 407	Glu 419–Arg 427	
WT	+	+	2.1	+	−	20.50
Radlowo	−	−	8.0	+	−	22.77
Chinese-4	+	−	3.0	+	+	20.58
Canton	−	−	3.3	+	−	20.33
Chinese-4 + Canton	−	+	5.2	+	+	22.24

tests which measure G6PD enzyme activity may yield normal results if the majority of cells express the normal allele, masking the presence of deficiency. Consequently, identifying G6PD heterozygotes solely through phenotypic testing poses challenges, highlighting the potential for molecular analysis to offer an alternative approach. In this study, 16 females identified as heterozygous for G6PD deficiency displayed enzyme activity levels exceeding the 70% cutoff threshold, thereby classified as having normal G6PD activity according to quantitative phenotypic testing. Additionally, Chu et al. (2017) reported two cases of heterozygous G6PD-deficient females with *Plasmodium vivax* malaria. Despite being screened as normal by FST, these individuals experienced haemolysis requiring blood transfusion as a result of a higher primaquine dose [54]. A wide range of enzyme activity observed in heterozygous females has also been described in previous studies among different populations [23, 55, 56]. However, quantitative phenotypic test using a G6PD biosensor has proven to be a feasible tool for management and radical cure of *P. vivax* malaria in various regions, including Brazilian Amazon, Cambodia and Thailand [57–59].

While phenotypic tests remain a valuable tool for diagnosing G6PD deficiency, they may not provide conclusive results in several circumstances. In such cases, genotypic testing, which directly analyses the individual's DNA for

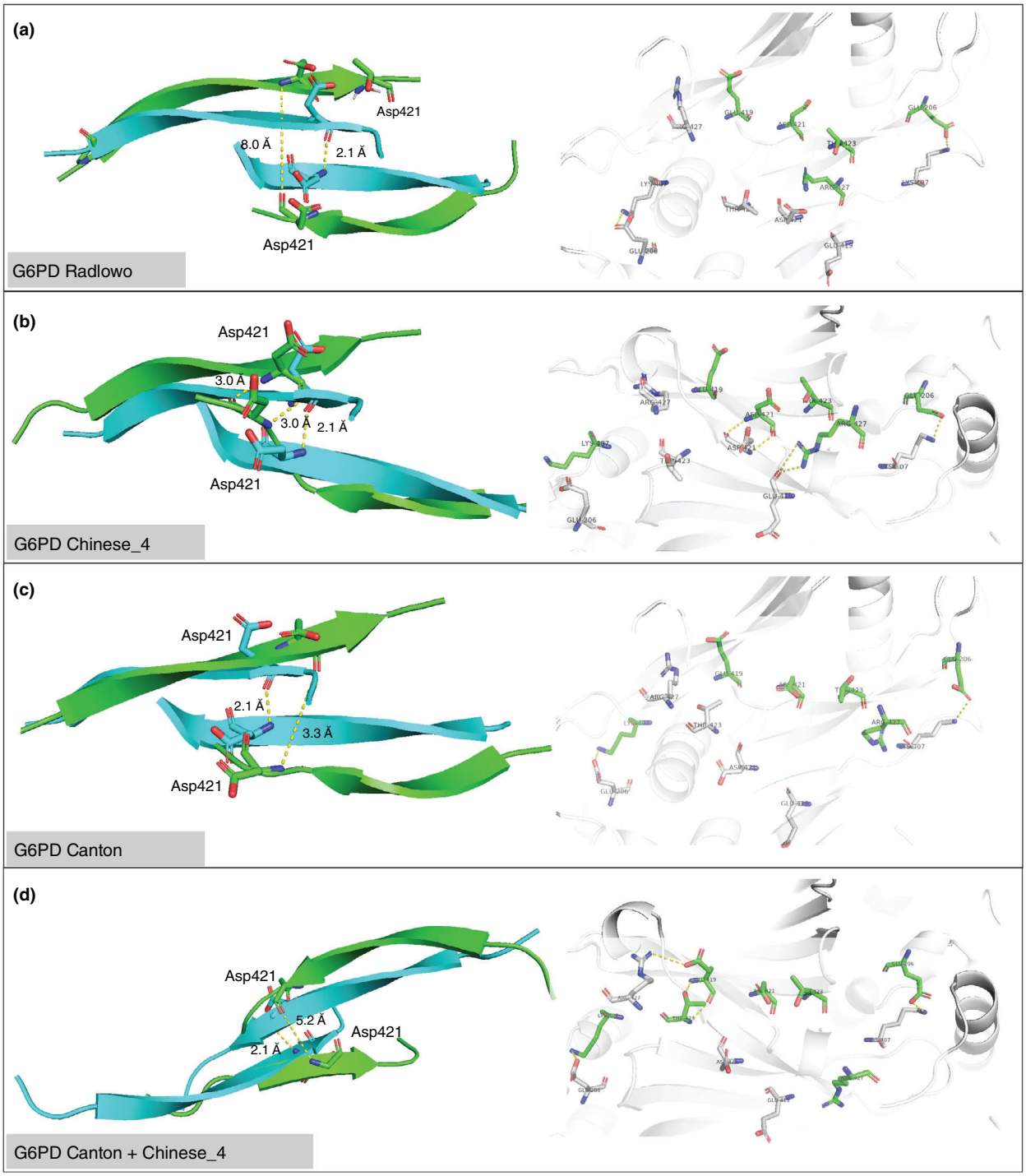

FIGURE 11 Dimer interface of G6PD variants and WT at 100 ns showing (on the left) the distance of βN-βN strands (res. 415–423) between chain A and chain B is higher in the variant (green) compared to the WT (cyan) and network interactions at the dimer interface (on the right) connecting residues in chain A (green) and chain B (grey) for (a) G6PD Radlowo, (b) G6PD Chinese-4, (c) G6PD Canton and (d) G6PD Chinese-4 + Canton.

G6PD gene mutations, can offer a more definitive diagnosis by identifying the presence of the deficient allele. The HRM assays developed here offered a high-throughput platform for detecting 15 *G6PD* mutations as well as identifying zygosity. The test is accurate and reliable, achieving 100% sensitivity and specificity for these mutations, with a run time of 80 min. While the assays were initially designed to target 15 *G6PD* mutations prevalent in Thailand and Southeast Asia, they were unable to identify six samples carrying *G6PD* Orissa, *G6PD* Radlowo and *G6PD* Kaiping, as these mutations were not included in assay panels. Therefore, expanding the assay to encompass

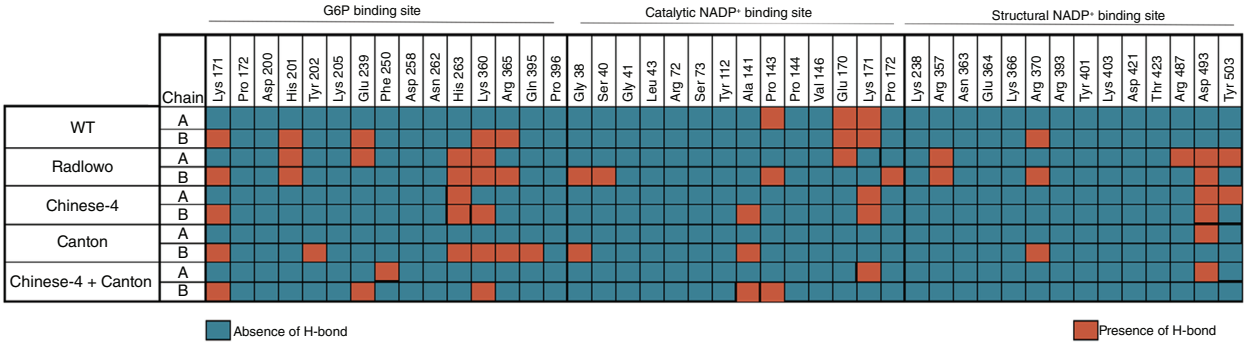

FIGURE 12 Ligand binding pocket occupancy indicating the presence (orange) and absence (turquoise) of hydrogen bonds.

additional mutations is necessary to ensure accuracy and adaptability. Despite this limitation, the developed assays present an advancement in improving G6PD deficiency diagnosis, not only in males with mild variants but also in identifying heterozygous females. By considering both phenotypic and genotypic test results, healthcare providers can more accurately diagnose G6PD deficiency and provide appropriate management and counselling for affected individuals and their families.

It should be noted that *G6PD* genetic testing alone could not provide information regarding haemolytic risk. However, genetic testing can still play a significant role in complementing phenotypic screening methods for G6PD deficiency. Genetic testing allows for better management of the condition in affected individuals, as they can be identified early and monitored for potential complications, such as haemolytic episodes triggered by certain medications or infections. Moreover, *G6PD* genotyping offers benefits in genetic counselling for families. By understanding the specific genetic traits, the risk of passing on the mutation to future generations can be more accurately assessed, empowering families to make informed decisions about their reproductive health. Furthermore, genetic testing contributes to a more comprehensive understanding of the prevalence and distribution of G6PD deficiency in populations, which is essential for public health planning and intervention strategies.

The prevalence of G6PD deficiency of 6.10% in this study aligns with findings from previous reports [26, 27, 30, 31, 35]. The distribution of *G6PD* mutations is varied across different geographical regions, depending on ethnicity. Ten, 8, 12 and 12 different *G6PD* genotypes were detected in Bangkok, Kaotakiab, Laemchabang and Lopburi, respectively. The most common *G6PD* genotype in this study was a combination of synonymous and intronic mutations (c.1311C>T and c.1365-13T>C), for which the molecular mechanisms leading to enzyme deficiency remain unclear. This combined mutation could result in a broad spectrum of enzyme activity levels, spanning from deficient to intermediate and even normal in both males and females. Additionally, the intronic mutation (c.486-34delT) could give rise to deficient and normal phenotypes in females. Similarly, previous studies [30, 60, 61] have reported that synonymous and intronic mutations can result in a wide range of G6PD activity across various population groups. However, the variability in enzyme activity observed for these mutations could be influenced by sample compromise during phenotype testing. Therefore, further investigation is required to elucidate the molecular mechanisms underlying G6PD enzyme deficiency attributed to c.1311C>T, c.1365-13T>C and c.486-34delT.

Missense G6PD mutations are known to cause enzyme deficiency by altering catalytic activity and/or structural stability [39, 40, 62]. It was found that both G6PD Radlowo and G6PD Chinese-4 + Canton altered the catalytic activity of the enzyme via destabilisation of protein structure, characterised by changes at the dimer and tetramer interfaces. G6PD Radlowo was detected in a heterozygous female with intermediate enzyme activity of 5.91 U/gHb. Originally discovered in Polish populations, this variant was classified as severe G6PD deficiency due to the negligible residual enzyme activity (<0.1%) in affected individuals without chronic non-spherocytic haemolytic anaemia [63]. Biochemical characterisation revealed significant impact from the Radlowo mutation, causing a remarkable 22-fold reduction in catalytic activity compared to the WT enzyme. The mutation profoundly destabilised the protein structure, resulting in a considerable decrease in thermal stability and increased susceptibility to chemical denaturation and trypsin digestion. The results suggest that individuals carrying G6PD Radlowo might be at great risk of developing haemolytic anaemia upon exposure to oxidative stress. A combination of Chinese-4 and Canton mutations was observed in a heterozygous female with a deficient phenotype (enzyme activity 1.08 U/gHb). This double mutation resulted in being 12-fold less catalytically active than the WT enzyme. While the Chinese-4 mutation moderately affected enzyme activity, the Canton mutation resulted in severe enzyme deficiency. Evaluation of the dimer and tetramer interfaces demonstrates that the presence of hydrogen bonds and salt bridges at the dimer interface is important in preserving the enzyme dimeric state. The destabilisation of protein structure caused by the Canton mutation was attributed to the disruption of oligomeric interactions [24]. Given the deficient enzyme

activity in individuals carrying this double mutation, it suggests that they may be more susceptible to haemolysis under oxidative stress.

In summary, the study provides comprehensive insights into the distribution, detection and characterisation of *G6PD* mutations, shedding light on their impact on enzyme function and stability. These findings carry significant implications for the diagnosis of G6PD deficiency. The development of HRM assays presented here offers a potential improvement in diagnostic techniques, enhancing the detection of G6PD deficiency in both males and females, particularly heterozygous females. This advancement holds great promise for improving patient care, facilitating genetic counselling and guiding public health initiatives aimed at addressing G6PD deficiency.

ACKNOWLEDGEMENTS

This research was supported by Mahidol University (Fundamental Fund: fiscal year 2024 by National Science Research and Innovation Fund [NSRF]) to UB. BACJ acknowledges the Department of Science and Technology—Philippine Council for Health Research and Development (DOST-PCHRD).

CONFLICT OF INTEREST STATEMENT

The authors declare no competing interests.

ORCID

Usa Boonyuen https://orcid.org/0000-0003-0640-6215

REFERENCES

1. Beutler E. Glucose-6-phosphate dehydrogenase: new perspectives. Blood. 1989;73(6):1397–401.
2. Motulsky AG. Metabolic polymorphisms and the role of infectious diseases in human evolution. 1960. Hum Biol. 1989;61(5–6):835–69; discussion 70–7.
3. Luzzatto L, Ally M, Notaro R. Glucose-6-phosphate dehydrogenase deficiency. Blood. 2020;136:1225–40.
4. Eggleston LV, Krebs HA. Regulation of the pentose phosphate cycle. Biochem J. 1974;138(3):425–35.
5. Gaetani GF, Rolfo M, Arena S, Mangerini R, Meloni GF, Ferraris AM. Active involvement of catalase during hemolytic crises of favism. Blood. 1996;88(3):1084–8.
6. Gammal RS, Pirmohamed M, Somogyi AA, Morris SA, Formea CM, Elchynski AL, et al. Expanded clinical pharmacogenetics implementation consortium guideline for medication use in the context of G6PD genotype. Clin Pharmacol Ther. 2023;113(5):973–85.
7. Singh H. Glucose-6-phosphate dehydrogenase deficiency: a preventable cause of mental retardation. Br Med J (Clin Res Ed). 1986; 292(6517):397–8.
8. World Health Organization. Test for glucose-6-phosphate dehydrogenase activity: target product profiles. Geneva: World Health Organization; 2022.
9. World Health Organization. Standardization of procedures for the study of glucose-6-phosphate dehydrogenase. Geneva: World Health Organization; 1967.
10. Sadhewa A, Cassidy-Seyoum S, Acharya S, Devine A, Price RN, Mwaura M, et al. A review of the current status of G6PD deficiency testing to guide radical cure treatment for vivax malaria. Pathogens. 2023;12(5):650.
11. Beutler E, Yeh M, Fairbanks VF. The normal human female as a mosaic of X-chromosome activity: studies using the gene for C-6-PD-deficiency as a marker. Proc Natl Acad Sci USA. 1962;48(1):9–16.
12. Luzzatto L, Nannelli C, Notaro R. Glucose-6-phosphate dehydrogenase deficiency. Hematol Oncol Clin North Am. 2016;30(2): 373–93.
13. Harper PS. Mary Lyon and the hypothesis of random X chromosome inactivation. Hum Genet. 2011;130(2):169–74.
14. Chu CS, Bancone G, Soe NL, Carrara VI, Gornsawun G, Nosten F. The impact of using primaquine without prior G6PD testing: a case series describing the obstacles to the medical management of haemolysis. Wellcome Open Res. 2019;4:25.
15. Wong FL, Ithnin A, Othman A, Cheah FC. Glucose-6-phosphate dehydrogenase (G6PD)-deficient infants: enzyme activity and gene variants as risk factors for phototherapy in the first week of life. J Paediatr Child Health. 2017;53(7):705–10.
16. D'Urso M, Luzzatto L, Perroni L, Ciccodicola A, Gentile G, Peluso I, et al. An extensive search for RFLP in the human glucose-6-phosphate dehydrogenase locus has revealed a silent mutation in the coding sequence. Am J Hum Genet. 1988;42(5):735–41.
17. Maffi D, Pasquino MT, Caprari P, Caforio MP, Cianciulli P, Sorrentino F, et al. Identification of G6PD Mediterranean mutation by amplification refractory mutation system. Clin Chim Acta. 2002; 321(1–2):43–7.
18. Yan JB, Xu HP, Xiong C, Ren ZR, Tian GL, Zeng F, et al. Rapid and reliable detection of glucose-6-phosphate dehydrogenase (G6PD) gene mutations in Han Chinese using high-resolution melting analysis. J Mol Diagn. 2010;12(3):305–11.
19. Twist GP, Gaedigk R, Leeder JS, Gaedigk A. High-resolution melt analysis to detect sequence variations in highly homologous gene regions: application to CYP2B6. Pharmacogenomics. 2013;14(8): 913–22.
20. Thomas V, Mazard B, Garcia C, Lacan P, Gagnieu MC, Joly P. UGT1A1 (TA)n genotyping in sickle-cell disease: high resolution melting (HRM) curve analysis or direct sequencing, what is the best way? Clin Chim Acta. 2013;424:258–60.
21. Fan Z, Weng X, Huang G, Pan Z, Long Z, Fan Q, et al. STARD-rapid screening for the 6 most common G6PD gene mutations in the Chinese population using the amplification refractory mutation system combined with melting curve analysis. Medicine (Baltimore). 2018; 97(17):e0426.
22. Islam MT, Sarker SK, Talukder S, Bhuyan GS, Rahat A, Islam NN, et al. High resolution melting curve analysis enables rapid and reliable detection of G6PD variants in heterozygous females. BMC Genet. 2018;19(1):58.
23. Boonyuen U, Songdej D, Tanyaratsrisakul S, Phuanukoonnon S, Chamchoy K, Praoparotai A, et al. Glucose-6-phosphate dehydrogenase mutations in malaria endemic area of Thailand by multiplexed high-resolution melting curve analysis. Malar J. 2021;20(1):194.
24. Boonyuen U, Jacob BAC, Wongwigkan J, Chamchoy K, Singha-Art N, Pengsuk N, et al. Genetic analysis and molecular basis of G6PD deficiency among malaria patients in Thailand: implications for safe use of 8-aminoquinolines. Malar J. 2024;23(1):38.
25. Tanphaichitr VS, Pung-amritt P, Yodthong S, Soongswang J, Mahasandana C, Suvatte V. Glucose-6-phosphate dehydrogenase deficiency in the newborn: its prevalence and relation to neonatal jaundice. Southeast Asian J Trop Med Public Health. 1995;26(Suppl 1): 137–41.
26. Nuchprayoon I, Sanpavat S, Nuchprayoon S. Glucose-6-phosphate dehydrogenase (G6PD) mutations in Thailand: G6PD Viangchan (871G>A) is the most common deficiency variant in the Thai population. Hum Mutat. 2002;19(2):185.
27. Laosombat V, Sattayasevana B, Janejindamai W, Viprakasit V, Shirakawa T, Nishiyama K, et al. Molecular heterogeneity of glucose-6-phosphate dehydrogenase (G6PD) variants in the south of Thailand and identification of a novel variant (G6PD Songklanagarind). Blood Cells Mol Dis. 2005;34(2):191–6.
28. Ninokata A, Kimura R, Samakkarn U, Settheetham-Ishida W, Ishida T. Coexistence of five G6PD variants indicates ethnic complexity of Phuket islanders, southern Thailand. J Hum Genet. 2006;51(5): 424–8.

29. Charoenkwan P, Tantiprabha W, Sirichotiyakul S, Phusua A, Sanguansermsri T. Prevalence and molecular characterization of glucose-6-phosphate dehydrogenase deficiency in northern Thailand. Southeast Asian J Trop Med Public Health. 2014;45(1):187–93.
30. Chamchoy K, Sudsumrit S, Wongwigkan J, Petmitr S, Songdej D, Adams ER, et al. Molecular characterization of G6PD mutations identifies new mutations and a high frequency of intronic variants in Thai females. PLoS One. 2023;18(11):e0294200.
31. Phompradit P, Kuesap J, Chaijaroenkul W, Rueangweerayut R, Hongkaew Y, Yamnuan R, et al. Prevalence and distribution of glucose-6-phosphate dehydrogenase (G6PD) variants in Thai and Burmese populations in malaria endemic areas of Thailand. Malar J. 2011;10:368.
32. Banyatsuppasin W, Jindadamrongwech S, Limrungsikul A, Butthep P. Prevalence of thalassemia and glucose-6-phosphate dehydrogenase deficiency in newborns and adults at the Ramathibodi Hospital, Bangkok, Thailand. Hemoglobin. 2017;41(4–6):260–6.
33. Dechyotin S, Sakunthai K, Khemtonglang N, Yamsri S, Sanchaisuriya K, Kitcharoen K, et al. Prevalence and molecular characterization of glucose-6-phosphate dehydrogenase (G6PD) deficiency in females from previously malaria endemic regions in northeastern Thailand and identification of a novel G6PD variant. Mediterr J Hematol Infect Dis. 2021;13(1):e2021029.
34. Sathupak S, Leecharoenkiat K, Kampuansai J. Prevalence and molecular characterization of glucose-6-phosphate dehydrogenase deficiency in the Lue ethnic group of northern Thailand. Sci Rep. 2021;11(1):2956.
35. Nuinoon M, Krithong R, Pramtong S, Sasuk P, Ngeaiad C, Chaimusik S, et al. Prevalence of G6PD deficiency and G6PD variants amongst the southern Thai population. PeerJ. 2022;10:e14208.
36. Thedsawad A, Wanachiwanawin W, Taka O, Hantaweepant C. Cut-off values for diagnosis of G6PD deficiency by flow cytometry in Thai population. Ann Hematol. 2022;101(10):2149–57.
37. Nannelli C, Bosman A, Cunningham J, Dugue PA, Luzzatto L. Genetic variants causing G6PD deficiency: clinical and biochemical data support new WHO classification. Br J Haematol. 2023;202(5):1024–32.
38. Gomez-Manzo S, Terron-Hernandez J, de la Mora- Mora I, Gonzalez-Valdez A, Marcial-Quino J, Garcia-Torres I, et al. The stability of G6PD is affected by mutations with different clinical phenotypes. Int J Mol Sci. 2014;15(11):21179–201.
39. Pakparnich P, Sudsumrit S, Imwong M, Suteewong T, Chamchoy K, Pakotiprapha D, et al. Combined effects of double mutations on catalytic activity and structural stability contribute to clinical manifestations of glucose-6-phosphate dehydrogenase deficiency. Sci Rep. 2021;11(1):24307.
40. Geck RC, Powell NR, Dunham MJ. Functional interpretation, cataloging, and analysis of 1,341 glucose-6-phosphate dehydrogenase variants. Am J Hum Genet. 2023;110(2):228–39.
41. Tantular IS, Kawamoto F. An improved, simple screening method for detection of glucose-6-phosphate dehydrogenase deficiency. Trop Med Int Health. 2003;8(6):569–74.
42. Chamchoy K, Praoparotai A, Pakparnich P, Sudsumrit S, Swangsri T, Chamnanchanunt S, et al. The integrity and stability of specimens under different storage conditions for glucose-6-phosphate dehydrogenase deficiency screening using WST-8. Acta Trop. 2021;217:105864.
43. Domingo GJ, Satyagraha AW, Anvikar A, Baird K, Bancone G, Bansil P, et al. G6PD testing in support of treatment and elimination of malaria: recommendations for evaluation of G6PD tests. Malar J. 2013;12:391.
44. World Health Organization. Testing for G6PD deficiency for safe use of primaquine in radical cure of *P. vivax* and *P. ovale* malaria. Geneva: WHO; 2016.
45. Sudsumrit S, Chamchoy K, Songdej D, Adisakwattana P, Krudsood S, Adams ER, et al. Genotype-phenotype association and biochemical analyses of glucose-6-phosphate dehydrogenase variants: implications for the hemolytic risk of using 8-aminoquinolines for radical cure. Front Pharmacol. 2022;13:1032938. https://doi.org/10.3389/fphar.2022.1032938
46. Au SW, Gover S, Lam VM, Adams MJ. Human glucose-6-phosphate dehydrogenase: the crystal structure reveals a structural NADP(+) molecule and provides insights into enzyme deficiency. Structure. 2000;8(3):293–303.
47. Louis NE, Hamza MA, Engku Baharuddin PNSD, Chandran S, Latif NA, Alonazi MA, et al. Assessing the structural dynamics of the glucose-6-phosphate dehydrogenase dimer interface using molecular dynamics simulation and ligand screening using computer aided drug discovery. Mol Simul. 2023;50(1):63–74. https://doi.org/10.1080/08927022.2023.2274871
48. Malde AK, Zuo L, Breeze M, Stroet M, Poger D, Nair PC, et al. An automated force field topology builder (ATB) and repository: version 1.0. J Chem Theory Comput. 2011;7(12):4026–37.
49. Pronk S, Pall S, Schulz R, Larsson P, Bjelkmar P, Apostolov R, et al. GROMACS 4.5: a high-throughput and highly parallel open source molecular simulation toolkit. Bioinformatics. 2013;29(7):845–54.
50. Chu CS, Bancone G, Nosten F, White NJ, Luzzatto L. Primaquine-induced haemolysis in females heterozygous for G6PD deficiency. Malar J. 2018;17(1):101.
51. Rueangweerayut R, Bancone G, Harrell EJ, Beelen AP, Kongpatanakul S, Mohrle JJ, et al. Hemolytic potential of tafenoquine in female volunteers heterozygous for glucose-6-phosphate dehydrogenase (G6PD) deficiency (G6PD mahidol variant) versus G6PD-normal volunteers. Am J Trop Med Hyg. 2017;97(3):702–11.
52. Beutler E. G6PD: population genetics and clinical manifestations. Blood Rev. 1996;10(1):45–52.
53. Lee HY, Ithnin A, Azma RZ, Othman A, Salvador A, Cheah FC. Glucose-6-phosphate dehydrogenase deficiency and neonatal hyperbilirubinemia: insights on pathophysiology, diagnosis, and gene variants in disease heterogeneity. Front Pediatr. 2022;10:875877.
54. Chu CS, Bancone G, Moore KA, Win HH, Thitipanawan N, Po C, et al. Haemolysis in G6PD heterozygous females treated with primaquine for plasmodium vivax malaria: a nested cohort in a trial of radical curative regimens. PLoS Med. 2017;14(2):e1002224.
55. Powers JL, Best DH, Grenache DG. Genotype–phenotype correlations of glucose-6-phosphate–deficient variants throughout an activity distribution. J Appl Lab Med. 2018;2(6):841–50.
56. He Y, Zhang Y, Chen X, Wang Q, Ling L, Xu Y. Glucose-6-phosphate dehydrogenase deficiency in the Han Chinese population: molecular characterization and genotype-phenotype association throughout an activity distribution. Sci Rep. 2020;10(1):17106.
57. Brito M, Rufatto R, Murta F, Sampaio V, Balieiro P, Baia-Silva D, et al. Operational feasibility of *Plasmodium vivax* radical cure with tafenoquine or primaquine following point-of-care, quantitative glucose-6-phosphate dehydrogenase testing in the Brazilian Amazon: a real-life retrospective analysis. Lancet Glob Health. 2024;12(3):e467–77.
58. Cassidy-Seyoum SA, Chheng K, Chanpheakdey P, Meershoek A, Hsiang MS, von Seidlein L, et al. Implementation of glucose-6-phosphate dehydrogenase (G6PD) testing for plasmodium vivax case management, a mixed method study from Cambodia. PLOS Glob Public Health. 2024;4(7):e0003476.
59. Bancone G, Gilder ME, Win E, Gornsawun G, Penpitchaporn P, Moo PK, et al. Technical evaluation and usability of a quantitative G6PD POC test in cord blood: a mixed-methods study in a low-resource setting. BMJ Open. 2022;12(12):e066529.
60. Shen S, Xiong Q, Cai W, Hu R, Zhou B, Hu X. Molecular heterogeneity of glucose-6-phosphate dehydrogenase deficiency in neonates in Wuhan: description of four novel variants. Front Genet. 2022;13:994015.
61. Lin F, Lou ZY, Xing SY, Zhang L, Yang LY. The gene spectrum of glucose-6-phosphate dehydrogenase (G6PD) deficiency in Guangdong province, China. Gene. 2018;678:312–7.

62. Boonyuen U, Chamchoy K, Swangsri T, Saralamba N, Day NP, Imwong M. Detailed functional analysis of two clinical glucose-6-phosphate dehydrogenase (G6PD) variants, G6PDViangchan and G6PDViangchan+Mahidol: decreased stability and catalytic efficiency contribute to the clinical phenotype. Mol Genet Metab. 2016;118(2): 84–91.
63. Jablonska-Skwiecinska E, Lewandowska I, Plochocka D, Topczewski J, Zimowski JG, Klopocka J, et al. Several mutations including two novel mutations of the glucose-6-phosphate dehydrogenase gene in polish G6PD deficient subjects with chronic nonspherocytic hemolytic anemia, acute hemolytic anemia, and favism. Hum Mutat. 1999;14(6): 477–84.

How to cite this article: Boonyuen U, Jacob BAC, Chamchoy K, Pengsuk N, Talukam S, Petcharat C, et al. Improved genetic screening with zygosity detection through multiplex high-resolution melting curve analysis and biochemical characterisation for G6PD deficiency. Trop Med Int Health. 2025. https://doi.org/10.1111/tmi.14105